

April 2009  
Version 2.03

Scintec Boundary Layer Scintillometer

# Hardware Manual

**BLS450**  
**BLS900**  
**BLS2000**

(including BLSDMI-1 option)



Scintec AG  
Wilhelm-Maybach-Str. 14  
72108 Rottenburg  
Germany

Tel [+49]-7472-98643-0  
Fax [+49]-7472-9808714  
E-Mail [info@scintec.com](mailto:info@scintec.com)  
[www.scintec.com](http://www.scintec.com)





---

## Contents

<b>1</b>	<b>INTRODUCTION.....</b>	<b>1</b>
1.1	FEATURES .....	1
1.2	DESCRIPTION .....	1
<b>2</b>	<b>QUICK REFERENCE GUIDE.....</b>	<b>3</b>
<b>3</b>	<b>HARDWARE PREPARATIONS .....</b>	<b>4</b>
3.1	SELECTION OF PATH AND SITE .....	4
3.1.1	PROPAGATION PATH .....	4
3.1.2	PATH HEIGHT .....	4
3.1.3	SITE REQUIREMENTS .....	5
3.1.4	RECOMMENDED PATH LENGTH AND HEIGHT .....	5
3.2	INSTALLING THE INSTRUMENTS .....	6
3.2.1	TRANSMITTER SET-UP.....	6
3.2.2	RECEIVER AND SPU SET-UP .....	7
3.2.3	RECEIVER DIP SWITCH SETTINGS .....	7
3.3	ALIGNMENT.....	9
3.3.1	TRANSMITTER ALIGNMENT .....	9
3.3.2	RECEIVER ALIGNMENT .....	9
3.4	RECOMMENDATIONS .....	10
<b>4</b>	<b>HARDWARE.....</b>	<b>11</b>
4.1	TRANSMITTER.....	11
4.1.1	OVERVIEW .....	11
4.1.2	APPLIANCE .....	11
4.2	RECEIVER .....	13
4.2.1	OVERVIEW .....	13
4.2.2	APPLIANCE .....	14
4.3	SIGNAL PROCESSING UNIT (SPU) .....	14
4.3.1	OVERVIEW .....	14
4.3.2	POWER SUPPLY.....	16
4.3.3	CONNECTORS.....	16
4.3.4	CURRENTS ON WEATHER STATION PORTS AND ANALOG OUT .....	19
4.3.5	WEATHER STATION CABLE WITH PC CONNECTOR.....	19
4.3.6	WEATHER STATION CABLE WITH DATALOGGER CONNECTOR (OPTIONAL) .....	20
4.3.7	WEATHER STATION CABLE WITH OPEN WIRES (OPTIONAL) .....	20
4.3.8	ANALOG OUT CABLE WITH OPEN WIRES (OPTIONAL) .....	21
4.4	BLS POWER SUPPLY (OPTIONAL) .....	22
4.5	BLS UNINTERRUPTIBLE POWER SUPPLY (OPTIONAL).....	22
4.6	DIRECT METEOROLOGICAL INPUT BLSDMI-1 (OPTIONAL).....	23
4.6.1	OVERVIEW .....	23
4.6.2	APPLIANCE .....	23
4.7	BLS2000 RECEIVER HEATING (OPTIONAL).....	25
4.8	PATH REDUCTION APERTURE (OPTIONAL).....	25
4.8.1	RECEIVER PATH REDUCTION APERTURES .....	25
4.8.2	TRANSMITTER PATH REDUCTION APERTURES .....	26
<b>APPENDIX A</b>	<b>THEORY .....</b>	<b>28</b>
A.1	OVERVIEW .....	28
A.2	MEASUREMENTS UNDER CONDITIONS OF WEAK SCATTERING .....	28
A.3	MEASUREMENTS UNDER CONDITIONS OF STRONG SCATTERING .....	31
A.4	ABSORPTION FLUCTUATIONS .....	32

---

A.5	WEIGHTING FUNCTIONS.....	33
A.5.1	TABULAR VALUES OF SPECTRAL WEIGHTING FUNCTION .....	36
A.5.2	TABULAR VALUES OF PATH WEIGHTING FUNCTION.....	37
A.5.3	ANALYTIC APPROXIMATION OF PATH WEIGHTING FUNCTION .....	38
A.6	RELATION TO OTHER TURBULENCE STATISTICS.....	39
A.7	MEASUREMENT OF WIND SPEED.....	40
A.8	MEASUREMENT OF HEAT FLUX.....	40
A.9	REFERENCES.....	41
<b>APPENDIX B</b>	<b>TRANSMITTER AND RECEIVER DIMENSIONS.....</b>	<b>42</b>
B.1	TRANSMITTER.....	42
B.1.1	BLS450 TRANSMITTER.....	42
B.1.2	BLS900 TRANSMITTER.....	44
B.1.3	BLS2000 TRANSMITTER.....	46
B.2	RECEIVER.....	48
B.2.1	BLS450 / BLS900 RECEIVER.....	48
B.2.2	BLS2000 RECEIVER.....	50
<b>APPENDIX C</b>	<b>SPECIFICATIONS.....</b>	<b>52</b>
C.1	TRANSMITTER.....	52
C.2	RECEIVER.....	53
C.3	SPU.....	53
C.4	BLS POWER SUPPLY.....	54
C.5	BLS UPS.....	54
<b>APPENDIX D</b>	<b>DECLARATION OF CONFORMITY.....</b>	<b>55</b>

---

## List of Figures

Figure 1: Illustration of path length definition .....	4
Figure 2: Receiver side view .....	8
Figure 3: Dip switch inside the receiver tube (example illustrates the factory setting for a BLS900) 8	
Figure 4: Receiver positioning device .....	9
Figure 5: Receiver positioning device for BLS2000 .....	10
Figure 6: Transmitter front view, Left: BLS450, Right: BLS900/BLS2000 .....	11
Figure 7: Connectors at BLS Transmitter .....	12
Figure 8: BLS900 Receiver side view .....	13
Figure 9: BLS900 Receiver rear view .....	14
Figure 10: SPU front view .....	15
Figure 11: BLS Power Supply front view .....	22
Figure 12: BLS UPS front view .....	22
Figure 13: Electrical connections of the BLSDMI-1 sensors .....	24
Figure 14: BLS2000 Heating connector at SPU and corresponding pin signals .....	25
Figure 15: Receiver Path Reduction Aperture for BLS450 and BLS900 .....	26
Figure 16: Receiver Path Reduction Aperture for BLS2000 .....	26
Figure 17: Transmitter Path Reduction Aperture for BLS450 and BLS900 .....	26
Figure 18: Transmitter Path Reduction Aperture for BLS2000 .....	27
Figure 19: Relation between the log-amplitude B11 and the path length R3 for the BLS900 .....	30
Figure 20: Comparison of log-amplitude variances B11 including and excluding saturation .....	32
Figure 21: Relation between Q and the path length R3 for the BLS900 .....	33
Figure 22: Spectral weighting function for B11, path length is 1000m .....	34
Figure 23: Spectral weighting function for Q, path length is 1000m .....	34
Figure 24: Spatial weighting function for B11, path length is 1000m .....	35
Figure 25: Spatial weighting function for Q, path length is 1000m .....	35
Figure 26: BLS450 Transmitter – Front View .....	42
Figure 27: BLS450 Transmitter – Rear View .....	42
Figure 28: BLS450 Transmitter – Bottom View .....	43
Figure 29: BLS450 Transmitter – Side View .....	43
Figure 30: BLS900 Transmitter – Front View .....	44
Figure 31: BLS900 Transmitter – Rear View .....	44
Figure 32: BLS900 Transmitter – Bottom View .....	45
Figure 33: BLS900 Transmitter – Side View .....	45
Figure 34: BLS2000 Transmitter – Front View .....	46
Figure 35: BLS2000 Transmitter – Rear View .....	46
Figure 36: BLS2000 Transmitter – Bottom View .....	47
Figure 37: BLS2000 Transmitter – Side View .....	47
Figure 38: BLS450 / BLS900 Receiver – Front View .....	48
Figure 39: BLS450 / BLS900 Receiver– Rear View .....	48
Figure 40: BLS450 / BLS900 Receiver – Bottom View .....	49
Figure 41: BLS450 / BLS900 Receiver – Side View .....	49
Figure 42: BLS2000 Receiver – Front View .....	50
Figure 43: BLS2000 Receiver– Rear View .....	50
Figure 44: BLS2000 Receiver – Bottom View .....	51
Figure 45: BLS2000 Receiver – Side View .....	51

---

## List of Tables

Table 1: Measurement ranges of $C_n^2$ , $C_T^2$ and heat flux for BLS450, BLS900 and BLS2000 .....	6
Table 2: Transmitter Operation Time for BLS450, BLS900 and BLS2000.....	7
Table 3: Recommended dip switch settings for different measurement ranges .....	9
Table 4: Tabular values of spectral weighting function.....	36
Table 5: Tabular values of path weighting function.....	37
Table 6: Specifications of BLS Transmitter .....	52
Table 7: Specifications of BLS Receiver.....	53
Table 8: Specifications of BLS SPU.....	53
Table 9: Specifications of BLS Power Supply.....	54
Table 10: Specifications of BLS UPS.....	54

---

## Important User Information

### **Note on Hardware Manual:**

This manual is intended for customers who have purchased a Scintec Boundary Layer Scintillometer BLS and/or the BLSDMI Option. A careful reading of this manual is substantial for a proper use and safe operation of the BLS.

### **Warranty and Liability:**

Scintec guarantees that the product has been thoroughly tested. The warranty included in the conditions of delivery is valid only if the Boundary Layer Scintillometer, and where applicable the BLSDMI Option, has been installed and used according to the instructions supplied by Scintec.

Scintec shall in no event be liable for incidental or consequential damages resulting from the incorrect and faulty use of the product. Note that user made modifications might affect the validity of the CE declaration.

Scintec reserves the right to make modifications to the design and technical specifications of products without prior notice.

---

# 1 INTRODUCTION

## 1.1 FEATURES

The BLS series are sophisticated scintillometer systems for the evaluation of atmospheric scintillation caused by refractive index fluctuations<sup>1</sup>. Large apertures of the transmitter and receiver eliminate saturation and inner scale effects. The instruments have the following features:

- Transmitter with large emission angle
- Homogeneous emission due to a large number of radiation sources
- Pulsed transmission with selectable repetition rate
- Modulated radiation for elimination of background
- Extremely sensitive, shot noise limited detector unit
- Insensitive to transmitter vibrations due to the large emission angle
- Interference filter for use in direct sunlight
- Path length user defined
- Virtually no transmitter alignment necessary
- Rapid installation and alignment of receiver with positioning device
- Comprehensive error identification and correction
- Calculation of structure function constant  $C_n^2$  of refractive index fluctuations
- Calculation of structure function constant  $C_T^2$  of temperature fluctuations
- Calculation of Fried diameter  $r_o$
- Calculation of turbulent surface heat flux  $H_0$  under conditions of free convection
- Calculation of crosswind speed
- Rugged weather-resistant design
- Eye-safe emission

## 1.2 DESCRIPTION

The BLS450, BLS900 and BLS2000 consist of an optical transmitter, an optical receiver with positioning device, a signal processing unit (SPU) and a data evaluation software (SRun) for a Microsoft Windows<sup>®</sup> based operating system.

The BLS900 transmitter emits radiation through 924 light emitting diodes (LED) on two disks. The BLS450 transmitter uses one radiating disk only. The BLS2000 transmitter uses two disks, each equipped with 912 LEDs. The LEDs can be operated in 4 different pulse repetition rates from 1Hz to 125 Hz. A pulse rate of 125 Hz provides maximum accuracy and transverse wind speed measurement capability, whereas a pulse rate of 1 Hz results in very low power consumption. The two-disk configuration of the BLS900 and BLS2000 allows for a correction of absorption fluctuations which is performed in the SRun software and increases the accuracy of the measurement. The two-disk configuration also provides crosswind measurement capability.

In the receivers of the BLS450, BLS900 and BLS2000, radiation is collimated by a lens onto 2 photodiodes. The lens is of convex glass type for the BLS450 and BLS900. In order to minimize spherical aberration, the BLS2000 holds a Fresnel lens. One photodiode is used for sensing the turbulence-induced fluctuations, the auxiliary detector is used as an alignment aid. For alignment purposes the receiver is mounted on a 3 axis-positioning device and comes with a mounted

---

<sup>1</sup> Patent DE 19751144

---

telescope. The receiver electronics pre-amplifies and filters the signals. Transmitter and receiver can easily be mounted on standard tripods with 5/8-inch threads.

---

## 2 QUICK REFERENCE GUIDE

The following steps are required to perform a measurement:

1. Select path and site (Section 3.1)
2. Install the instruments (Section 3.2)
3. Install the software SRun (see Software Manual)
4. Select the device type and set all parameters in the Settings menu (see Software Manual)
5. Align the instruments (Sections 3.3 and Software Manual)
6. Start the measurement (see Software Manual)

---

## 3 HARDWARE PREPARATIONS

### 3.1 SELECTION OF PATH AND SITE

The propagation path length is defined as the distance between the glass window of the transmitter and the lens of the receiver (Figure 1)

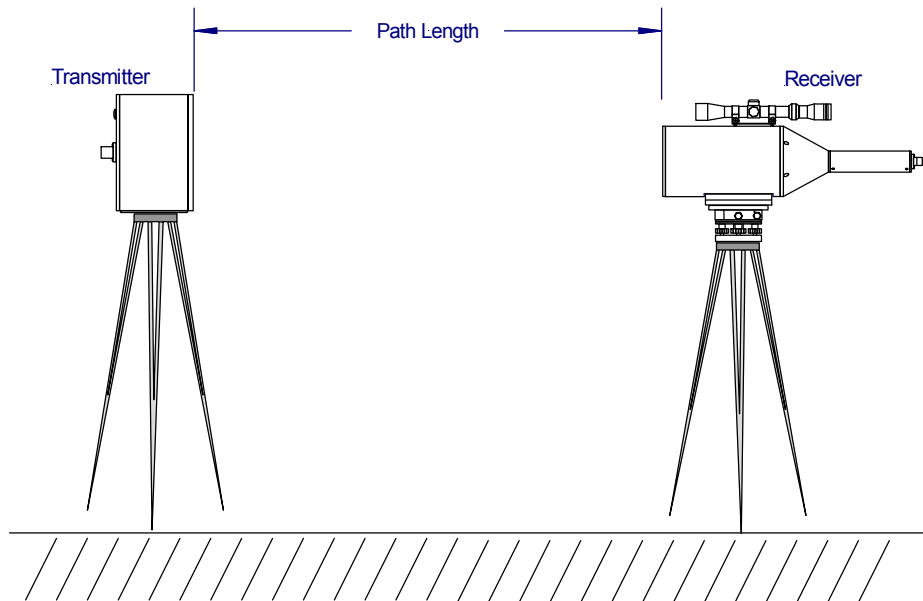


Figure 1: Illustration of path length definition

Operation of the BLS450 and BLS900 is possible over paths in the range 500 to 5000 m. The BLS2000 can be used from 1000m to 10000m.

After having chosen path and site

- the path length and height must be entered in the *Settings* menu of the SRun software
- the amplifier dip switch in the receiver unit must be set.

#### 3.1.1 PROPAGATION PATH

The ground along the propagation path should be as even as possible. A well defined measurement height is required for application of the free convection scaling for calculation of the turbulent sensible heat flux. Note that also the primarily measured quantities  $C_n^2$ , i.e. the structure function constant of refractive index fluctuations strongly depend on height.

A correction for slant paths is included in the SRUN software.

#### 3.1.2 PATH HEIGHT

The path height is defined as the height of the straight line connecting the transmitter and the receiver above ground. In case of a slant path the height of the transmitter and the receiver must be specified. If the surface is not totally flat, use the average height with an increased weight at the

path's centre. The path weighting functions (describing the contribution of different positions along the path) are given in Appendix A.5.

### 3.1.3 SITE REQUIREMENTS

The calculation of the turbulent heat flux is based on free convection scaling. The free convection scaling requires the measurement height to be significantly larger than the height of the roughness elements.

### 3.1.4 RECOMMENDED PATH LENGTH AND HEIGHT

For long propagation paths, saturation may occur under strong turbulence conditions. Saturation is avoided by using a sufficiently short propagation path or a large measurement height. In other words, larger path lengths suggest larger measurement heights.

The following table shows the measurement ranges of  $C_n^2$ ,  $C_T^2$  and heat flux for different path lengths. The ranges of  $C_T^2$  are provided assuming a pressure of 1013hPa. The turbulent heat flux ranges depend on the measurement height  $z$  in meters.

<b>BLS450</b>			
path length	$C_n^2$ [ $m^{-2/3}$ ]	$C_T^2$ [ $K^2 m^{-2/3}$ ]	heat flux [ $W/m^2$ ] at height $z$ [m]
500 m	$3 \times 10^{-14} - 1 \times 10^{-10}$	$3 \times 10^{-2} - 1 \times 10^{+2}$	$> 8 z$
1000 m	$4 \times 10^{-15} - 2 \times 10^{-11}$	$4 \times 10^{-3} - 2 \times 10^{+1}$	$2 z - 980 z$
2000 m	$4 \times 10^{-16} - 2 \times 10^{-12}$	$5 \times 10^{-4} - 2 \times 10^{+0}$	$0.5 z - 175 z$
3000 m	$1 \times 10^{-16} - 6 \times 10^{-13}$	$2 \times 10^{-4} - 7 \times 10^{-1}$	$0.2 z - 70 z$
5000 m	$3 \times 10^{-17} - 2 \times 10^{-13}$	$4 \times 10^{-5} - 2 \times 10^{-1}$	$0.05 z - 30 z$
<b>BLS450 with Path Reduction Aperture</b>			
path length	$C_n^2$ [ $m^{-2/3}$ ]	$C_T^2$ [ $K^2 m^{-2/3}$ ]	heat flux [ $W/m^2$ ] at height $z$ [m]
250 m	$5 \times 10^{-14} - 2 \times 10^{-10}$	$6 \times 10^{-2} - 2 \times 10^{+2}$	$> 12 z$
500 m	$6 \times 10^{-15} - 3 \times 10^{-11}$	$7 \times 10^{-3} - 4 \times 10^{+1}$	$2 z - 1500 z$
1000 m	$8 \times 10^{-16} - 6 \times 10^{-12}$	$9 \times 10^{-4} - 7 \times 10^{+0}$	$0.5 z - 400 z$
2000 m	$1 \times 10^{-16} - 6 \times 10^{-13}$	$1 \times 10^{-4} - 7 \times 10^{-1}$	$0.1 z - 70 z$
3000 m	$5 \times 10^{-17} - 2 \times 10^{-13}$	$6 \times 10^{-5} - 2 \times 10^{-1}$	$0.07 z - 30 z$
<b>BLS900</b>			
path length	$C_n^2$ [ $m^{-2/3}$ ]	$C_T^2$ [ $K^2 m^{-2/3}$ ]	heat flux [ $W/m^2$ ] at height $z$ [m]
500 m	$3 \times 10^{-14} - 3 \times 10^{-10}$	$3 \times 10^{-2} - 4 \times 10^{+2}$	$> 8 z$
1000 m	$4 \times 10^{-15} - 6 \times 10^{-11}$	$4 \times 10^{-3} - 7 \times 10^{+1}$	$2 z - 2400 z$
2000 m	$4 \times 10^{-16} - 6 \times 10^{-12}$	$5 \times 10^{-4} - 7 \times 10^{+0}$	$0.3 z - 412 z$
3000 m	$1 \times 10^{-16} - 3 \times 10^{-12}$	$2 \times 10^{-4} - 4 \times 10^{-1}$	$0.2 z - 270 z$
5000 m	$3 \times 10^{-17} - 6 \times 10^{-13}$	$4 \times 10^{-5} - 7 \times 10^{-1}$	$0.05 z - 75 z$

<b>BLS900 with Path Reduction Aperture</b>			
path length	$C_n^2$ [m <sup>-2/3</sup> ]	$C_T^2$ [K <sup>2</sup> m <sup>-2/3</sup> ]	heat flux [W/m <sup>2</sup> ] at height z [m]
250 m	$5 \times 10^{-14} - 1 \times 10^{-9}$	$6 \times 10^{-2} - 1 \times 10^{+3}$	> 12 z
500 m	$6 \times 10^{-15} - 2 \times 10^{-10}$	$7 \times 10^{-3} - 2 \times 10^{+2}$	2 z – 5500 z
1000 m	$8 \times 10^{-16} - 3 \times 10^{-11}$	$9 \times 10^{-4} - 4 \times 10^{+0}$	0.5 z – 1500 z
2000 m	$1 \times 10^{-16} - 6 \times 10^{-12}$	$1 \times 10^{-4} - 7 \times 10^{+0}$	0.1 z – 412 z
3000 m	$5 \times 10^{-17} - 2 \times 10^{-12}$	$6 \times 10^{-5} - 2 \times 10^{+0}$	0.07 z – 174 z
<b>BLS2000</b>			
path length	$C_n^2$ [m <sup>-2/3</sup> ]	$C_T^2$ [K <sup>2</sup> m <sup>-2/3</sup> ]	heat flux [W/m <sup>2</sup> ] at height z [m]
1000 m	$1 \times 10^{-14} - 1 \times 10^{-10}$	$2 \times 10^{-2} - 1 \times 10^{+2}$	5 z – 3600 z
2000 m	$2 \times 10^{-15} - 2 \times 10^{-11}$	$2 \times 10^{-3} - 2 \times 10^{+1}$	1 z – 980 z
3000 m	$5 \times 10^{-16} - 6 \times 10^{-12}$	$6 \times 10^{-4} - 7 \times 10^{+0}$	0.4 z – 413 z
5000 m	$1 \times 10^{-16} - 2 \times 10^{-12}$	$1 \times 10^{-4} - 2 \times 10^{+0}$	0.1 z – 175 z
7000 m	$4 \times 10^{-17} - 6 \times 10^{-13}$	$5 \times 10^{-5} - 7 \times 10^{-1}$	0.06 z – 73 z
10000 m	$2 \times 10^{-17} - 3 \times 10^{-13}$	$2 \times 10^{-5} - 4 \times 10^{-1}$	0.03 z – 48 z
<b>BLS2000 with Path Reduction Aperture</b>			
Path length	$C_n^2$ [m <sup>-2/3</sup> ]	$C_T^2$ [K <sup>2</sup> m <sup>-2/3</sup> ]	heat flux [W/m <sup>2</sup> ] at height z [m]
500 m	$3 \times 10^{-14} - 6 \times 10^{-10}$	$3 \times 10^{-2} - 7 \times 10^{+2}$	> 8 z
1000 m	$3 \times 10^{-15} - 1 \times 10^{-10}$	$4 \times 10^{-3} - 1 \times 10^{+2}$	2 z – 3575 z
2000 m	$4 \times 10^{-16} - 1 \times 10^{-11}$	$5 \times 10^{-4} - 1 \times 10^{+1}$	0.3 z – 635 z
3000 m	$1 \times 10^{-16} - 6 \times 10^{-12}$	$2 \times 10^{-4} - 7 \times 10^{+0}$	0.2 z – 412 z
5000 m	$8 \times 10^{-17} - 1 \times 10^{-12}$	$9 \times 10^{-5} - 1 \times 10^{+0}$	0.1 z – 113 z
7000 m	$1 \times 10^{-16} - 6 \times 10^{-13}$	$1 \times 10^{-4} - 7 \times 10^{-1}$	0.1 z – 73 z

Table 1: Measurement ranges of  $C_n^2$ ,  $C_T^2$  and heat flux for BLS450, BLS900 and BLS2000

## 3.2 INSTALLING THE INSTRUMENTS

The transmitter and the receiver units must be mounted on stable platforms. The required angular pointing stability is in the order of 0.1 mrad for the receiver. There is virtually no pointing stability required for the transmitter. The use of heavy tripods used for geodetic purposes is recommended. The 5/8-inch threads at the bottoms of the instruments allow an easy connection to such devices. Strong winds (around 10 m/s and more) may require additional means to ensure pointing stability and to avoid measurement errors caused by vibration of the transmitter or receiver.

### 3.2.1 TRANSMITTER SET-UP

The transmitter must be connected to an appropriate power supply (see specifications in APPENDIX C). A transmitter power supply cable is included. The power supply cable must not be prolonged as the additional resistance may cause instabilities in the switching power supply inside the transmitter. When using a battery as transmitter power supply the transmitter operation time is limited dependent on the transmitter pulse repetition rate (Table 2). The maximum operation time given is based on a battery capacity of 120 Ah. Larger capacities prolong operation time while lower capacities reduce it.

<b>BLS450 Transmitter Operation Time</b>		
Pulse Repetition Rate	Current Consumption (@12VDC)	Operation Time (C = 120 Ah)
1 Hz	0.075 A	> 8 weeks
5 Hz	0.25 A	> 2 weeks
25 Hz	0.8 A	> 6 days
125 Hz	3.5 A	> 30 hours
<b>BLS900 Transmitter Operation Time</b>		
Pulse Repetition Rate	Current Consumption (@12VDC)	Operation Time (C = 120 Ah)
1 Hz	0.15 A	> 4 weeks
5 Hz	0.5 A	> 1 weeks
25 Hz	1.6 A	> 3 days
125 Hz	7 A	> 15 hours
<b>BLS2000 Transmitter Operation Time</b>		
Pulse Repetition Rate	Current Consumption (@12VDC)	Operation Time (C = 120 Ah)
1 Hz	0.3 A	> 2 weeks
5 Hz	1 A	> 5 days
25 Hz	3 A	> 36 hours
125 Hz	13 A	> 8 hours

Table 2: Transmitter Operation Time for BLS450, BLS900 and BLS2000

The transmitter is switched on by pressing the red button at the back side (Figure 7). The green LED in the centre of the red button starts blinking at the same rate as the red LED's at the front side. With the red and the black button the pulse repetition rate can be set. The black button decreases the repetition rate while the red one increases it. The transmitter is switched off by pressing the red and the black button simultaneously.

If the supply voltage is cut off during operation the transmitter automatically starts with the last pulse repetition rate when the voltage is applied again. If the supply voltage is cut off while the transmitter is switched off it remains switched off when the voltage is applied again.

The red LED in the centre of the black button is also used as battery voltage control. The red LED blinks when the supply voltage drops below 9 V. A voltage of 9 V instead of 12 V reduces the signal 10 % at 25 Hz and 30 % at 1 Hz.

### 3.2.2 RECEIVER AND SPU SET-UP

The receiver is directly connected to and supplied by the SPU. The SPU requires a 12 V power supply (see specifications in APPENDIX C) and must be connected to a PC or network via the Ethernet cable link.

### 3.2.3 RECEIVER DIP SWITCH SETTINGS

Before starting the alignment or measurement the amplifier dip-switch inside the receiver must be set (Figure 2).

- Choose the correct settings for your measurement path from Table 3.
- Remove the three screws at the back part of the receiver unit.

- Pull out the rear panel, be careful not to damage the cables to the connector.

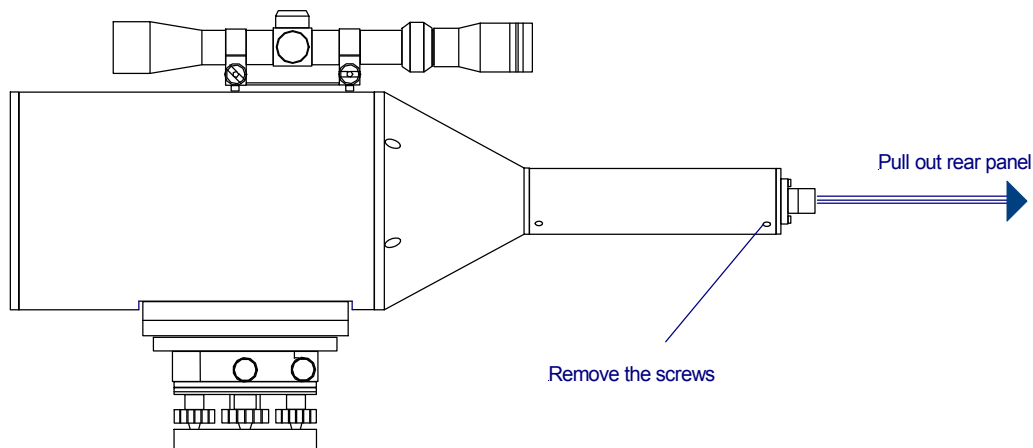


Figure 2: Receiver side view

Set the receiver dip switch according to Figure 3.

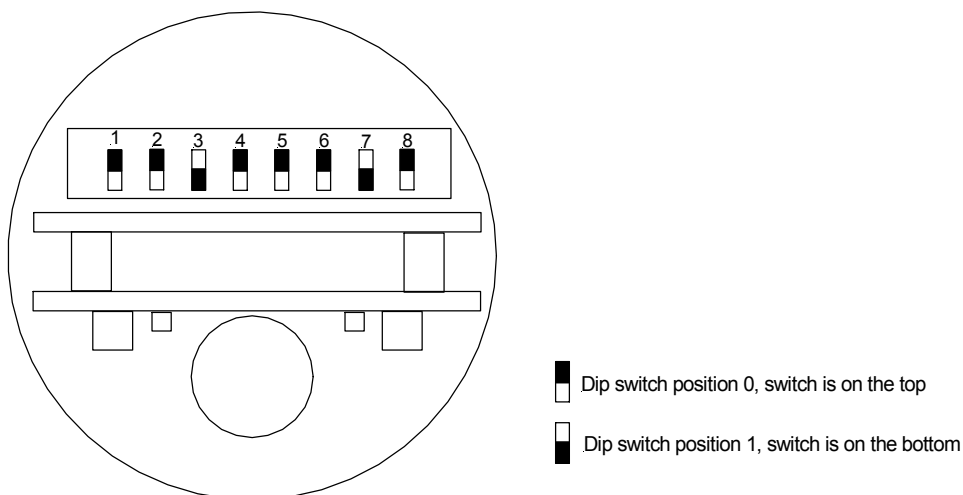


Figure 3: Dip switch inside the receiver tube (example illustrates the factory setting for a BLS900)

The software evaluates during a measurement relative changes of the intensity. Therefore, the adjustment of the signal levels has no direct effect on the accuracy of the results. However, the full measurement ranges (as provided in Table 1) can only be achieved if the measured signal levels of the X and Y channel remain within an optimum signal level range as indicated by SRun in the alignment mode. The signals of the channels XB and YB are the most relevant indicators for a proper alignment.

The signal heights depend on transmitter adjustment and temperature, receiver alignment and atmospheric transmission. If the signal is still too low or too high the next higher or lower amplification should be selected, respectively.

Measurement range	Dip switch BLS450/BLS900 1234 5678	Dip switch BLS2000 1234 5678
500 m – 750 m	1111 1111	n/a
750 m – 1500 m	0001 0001	1111 1111
1500 m – 2000 m	0110 0110	0001 0001
2000 m – 3000 m	0010 0010 (factory setting)	0110 0110
3000 m – 4000 m	0100 0100	0010 0010
4000 m – 5000 m	1000 1000	
5000 m – 8000 m	n/a	0100 0100 (factory setting)
8000 m – 10000 m	n/a	1000 1000

Table 3: Recommended dip switch settings for different measurement ranges

### 3.3 ALIGNMENT

To align the instruments the software SRUN must be installed (see software manual).

#### 3.3.1 TRANSMITTER ALIGNMENT

As the emission angle of the LED's is approximately 10° the transmitter has to be aligned only roughly to the direction where the receiver is located.

#### 3.3.2 RECEIVER ALIGNMENT

The receiver can be aligned to the direction of the transmitter by looking through the telescope and adjusting the positioning device until the transmitter is located at the centre of the crosshair. The magnification of the telescope can be varied from 3 to 9 by rotating the power ring.

##### **Positioning Device for BLS450 and BLS900**

The positioning device is equipped with 6 screws for adjustment (Figure 4). Screws 1 to 3 are for vertical adjustment, screws 4, 5 and 6 for adjusting the receiver in the horizontal. When screw 4 is tightened screws 5 and 6 can be used for small changes in the horizontal orientation. When screw 4 is loose the receiver can be rotated directly and screws 5 and 6 are not used.

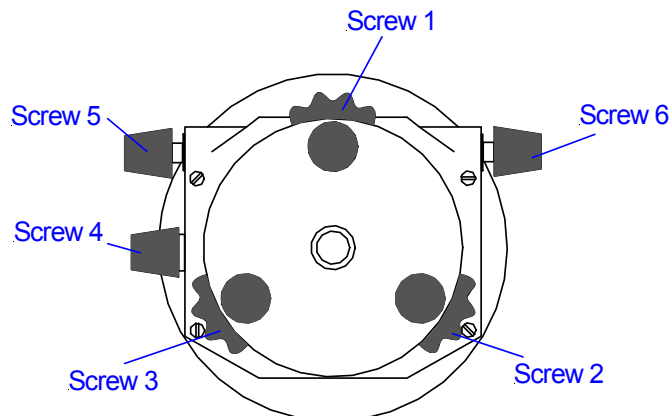


Figure 4: Receiver positioning device

---

### **Positioning Device for BLS2000**

The positioning device for the BLS2000 is equipped with 4 screws for adjustment (Figure 5). Screws 1 and 2 are for horizontal adjustment, whereas screws 3 and 4 allow an adjustment of the receiver in the vertical.

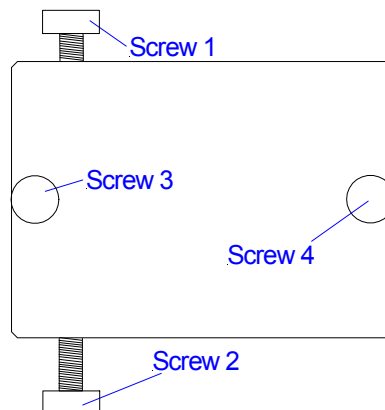


Figure 5: Receiver positioning device for BLS2000

For fine alignment the *Start* Option must be selected to start the alignment screen (= Alignment Mode). The signals in the alignment screen should be adjusted to a maximum by using the screws of the positioning device. As described in the software manual, the signals of the channels XB and YB are the most relevant indicators. It is recommended to iteratively adjust the receiver horizontally and vertically. Usually some iteration is necessary for optimal adjustment. If the signal levels are too low or too high, the amplifier dip-switch inside the receiver tube must be changed, respectively (see section 3.2.3).

When the received intensities are too small, check the following points:

- The transmitter is switched ON
- The transmitter power supply voltage exceeds 9V
- The SPU power supply is switched on and the supply voltage is 12 V
- The receiver unit is properly connected to the SPU

The RAM capacity of the SPU allows an operation of the receiver up to approximately 2 years, depending on the settings. When the amount of data exceeds the storage capacity, the next results are stored at the address of the first results, which will be overwritten (loop storage).

The only maintenance required will be to clean the windows and to check the status indicator LED. Re-adjust the alignment if necessary. The required re-alignment period depends on the stability of the mounting. With tripods, it mainly depends on the type and condition of the ground. With a concrete mounting, re-alignments will only rarely be necessary.

## **3.4 RECOMMENDATIONS**

In hot and sunny climates, the instruments (at least the transmitter) should be operated at a naturally ventilated place or a sun protection shield should be used to avoid overheating. The use of a metallic platform to mount the transmitter, e.g. aluminium tripods, is also recommended. Especially at a pulse repetition rate of 125 Hz the transmitter surface temperature can be 70°C – 80°C.

To avoid a high background signal the transmitter should be installed such that little radiation from the sky or the sun is seen from the receiver.

---

## 4 HARDWARE

The refractive index turbulence measurement system consists of an optical transmitter with tripod, an optical receiver with tripod and positioning device, a signal processing unit (SPU) and a data evaluation software for a PC.

### 4.1 TRANSMITTER

#### 4.1.1 OVERVIEW

The BLS900 transmitter emits radiation through 924 light emitting diodes (LED). It consists of two round cases, each housing a disk with 444 infrared and 18 red LEDs and two power supply boards. The BLS450 transmitter uses one radiating disk only and emits radiation through 462 LEDs. The BLS2000 transmitter uses two disks, each equipped with 878 infrared, 34 red LEDs and four power supply boards. A microcontroller board with overvoltage protection is included in the BLS450, BLS900 and BLS2000 transmitters. The LEDs can be operated in 4 different pulse repetition rates from 1Hz to 125 Hz. A pulse rate of 125 Hz provides maximum accuracy and transverse wind speed measurement capability, whereas a pulse rate of 1 Hz results in very low power consumption. The divergence of the emission is about 16°, therefore transmitter adjustment has to be done only very roughly.

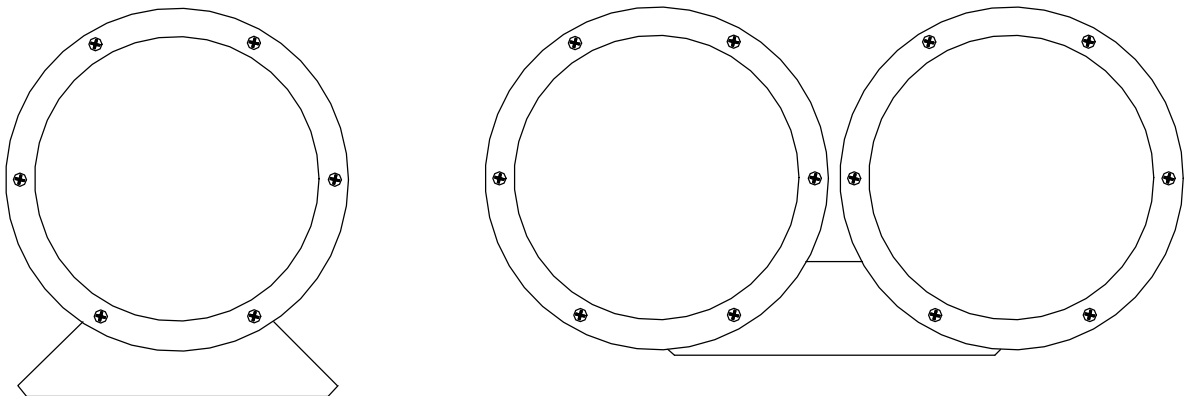


Figure 6: Transmitter front view, Left: BLS450, Right: BLS900/BLS2000

The 18 (34 for the BLS2000) red LED's on each disk work as an indicator for the correct function of the infrared LED's and show the current pulse repetition rate. Each red LED is connected with a segment consisting of 26 (27 for the BLS2000) infrared LED's.

Each LED disk emits pulses with a different modulation frequency: 1750 Hz for disk 1 (with the black and red buttons) and 2500 Hz for disk 2 (BLS900 and BLS2000).

#### 4.1.2 APPLIANCE

The transmitter is switched on by pressing the red button located on the rear panel of the transmitter (Figure 7). By pressing the button again, the pulse repetition rate is increased from 1 Hz to 5 Hz. By pressing the red button once again, the pulse repetition rate is increased from 5 Hz to 25 Hz, then to 125 Hz and then the pulse repetition rate starts from 1 Hz again. With the black button, the pulse group frequency is decreased in the same manner. The transmitter is switched off

by pressing the red and black button simultaneously. The pulse repetition rate is also indicated by the green LED in the red button.

Besides the red and black button, the back side of each transmitter hosts a connector for the power supply (Figure 7). The standard power supply cable has a length of 3 m.

In case of the BLS900 and BLS2000, the two rear panels are each equipped with an additional connector. The two LED disk boxes are connected via a short cable plugged into these connectors. The two connectors can be 4-pole or 7-pole.

The transmitter can easily be mounted on geodetic tripods using a thread adapter on the instruments bottom.

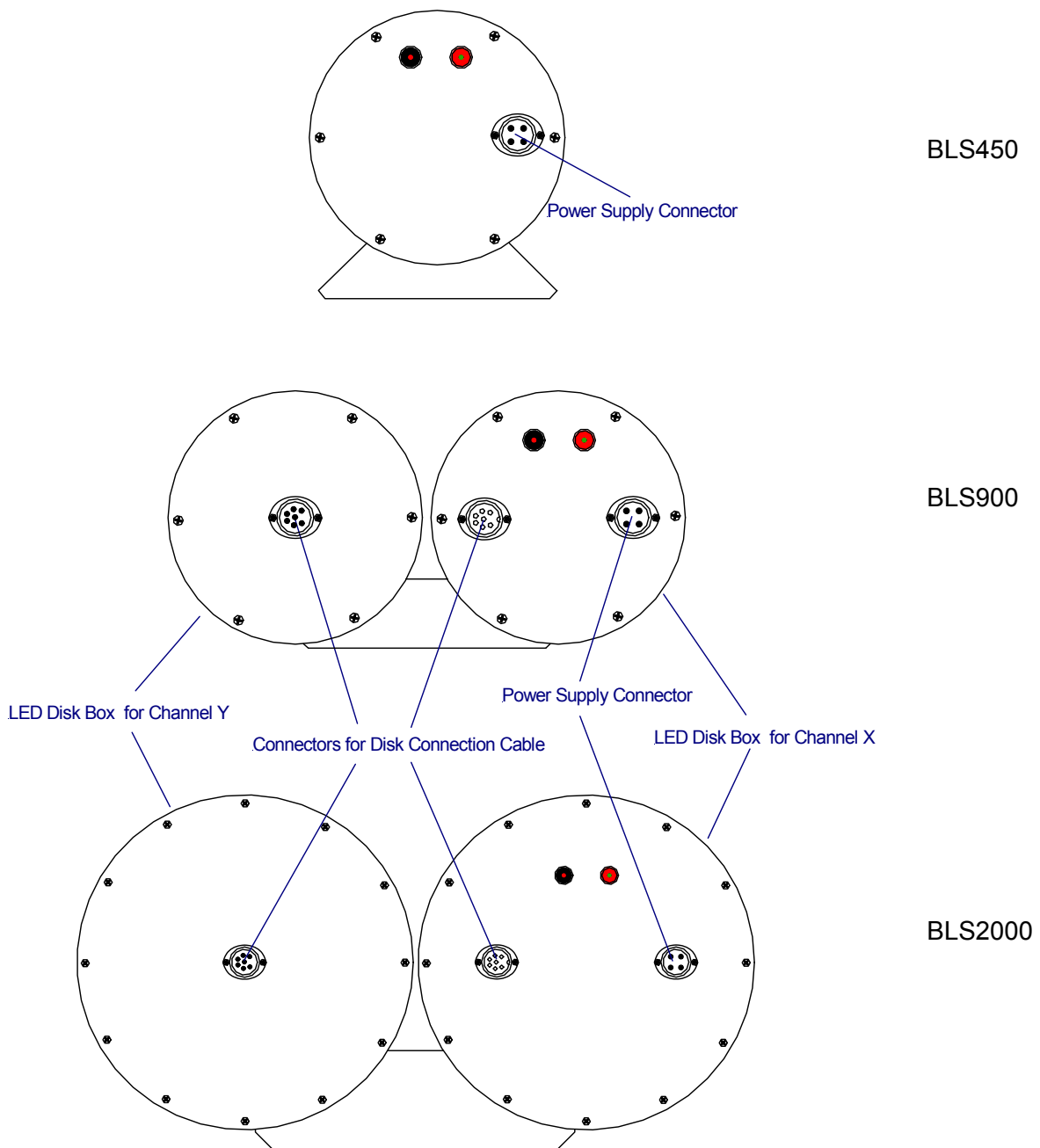


Figure 7: Connectors at BLS Transmitter

---

## 4.2 RECEIVER

### 4.2.1 OVERVIEW

With the BLS450 and BLS900, the modulated radiation is collimated by a plan convex lens ( $\varnothing = 145$  mm,  $f = 450$  mm) onto 2 Si photodiodes with different sensitive areas. The BLS2000 uses a Fresnel lens of 265 mm diameter and a focal length of 495 mm. The main detector on the optical axis is used for sensing the turbulence-induced fluctuations of the received modulated pulses. After demodulation the signals X and Y are available for the user during alignment. The auxiliary detector is used as an alignment aid. It provides the modulated signal Z.

The receiver (Figure 8) is held by a 3 axis-positioning device allowing easy alignment adjustments. A telescope is used to adjust the receiver's optical axis to the transmitter optically. The receiver can be mounted on geodetic tripods using a thread adapter on the instruments bottom.

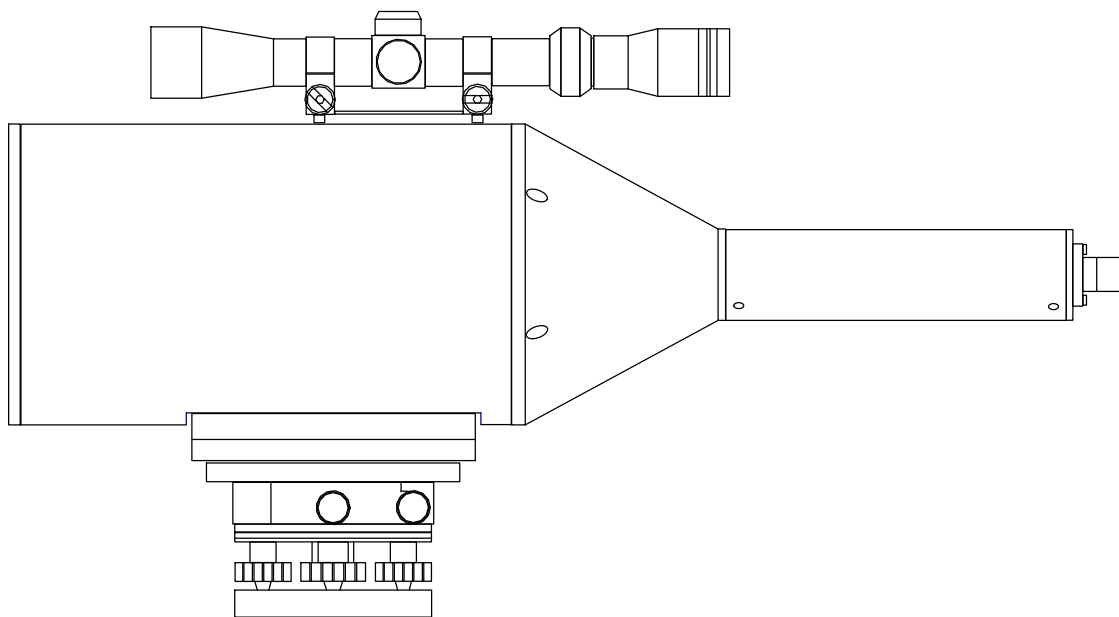


Figure 8: BLS900 Receiver side view

---

## 4.2.2 APPLIANCE

The receiver is connected to the SPU via a cable with a 9-pole-connector located on the rear panel of the receiver (Figure 9).

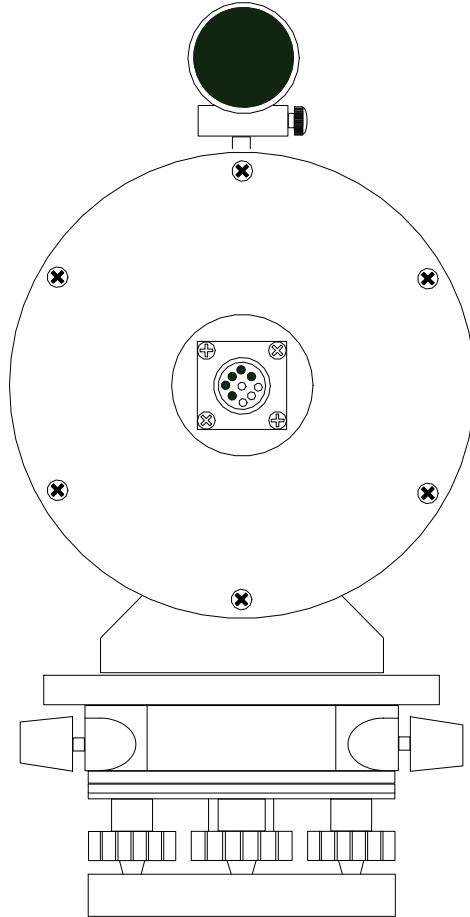


Figure 9: BLS900 Receiver rear view

## 4.3 SIGNAL PROCESSING UNIT (SPU)

### 4.3.1 OVERVIEW

The SPU is used for data acquisition and evaluation. It is directly connected to the receiver and communicates with the PC or a network via an Ethernet cable link. No connection is needed between receiver and transmitter. The pulse repetition rate is determined automatically.

The SPU contains a card for performing the filtering and demodulation of the signals X and Y. A microprocessor card governs further signal processing, calculating the results, storing the results and transferring the data via the Ethernet cable link to a PC or network.

The Signal processing unit also generates the  $\pm 12V$  voltages needed for the receiver from a single external +12V power supply.

The SPU is equipped with three LEDs. They give information about the following system properties:

<b>Power</b>	LED lights on green when proper voltage is applied to the system
<b>Status</b>	<p>LED lights on yellow as follows:</p> <ul style="list-style-type: none"> <li>- The status LED blinks with a period of 2 seconds after having powered on the BLS system. The system is now ready for starting a measurement</li> <li>- In measurement mode, the LED is continuously illuminated with short interrupts every second. This indicates a 90% duty cycle.</li> <li>- During start-up Status LED and Error LED blink alternatingly.</li> </ul>
<b>Error</b>	<p>The SPU is equipped with a Built-In-Test-Equipment including a voltage monitoring system. LED lights on red in the following cases:</p> <ul style="list-style-type: none"> <li>- In case of an internal malfunction, measurement error or external voltage drop, the LED lights on red permanently.</li> <li>- During start-up Status LED and Error LED blink alternatingly.</li> </ul>

The overall configuration of the LEDs as well as connectors on the SPU front side is illustrated in Figure 10.

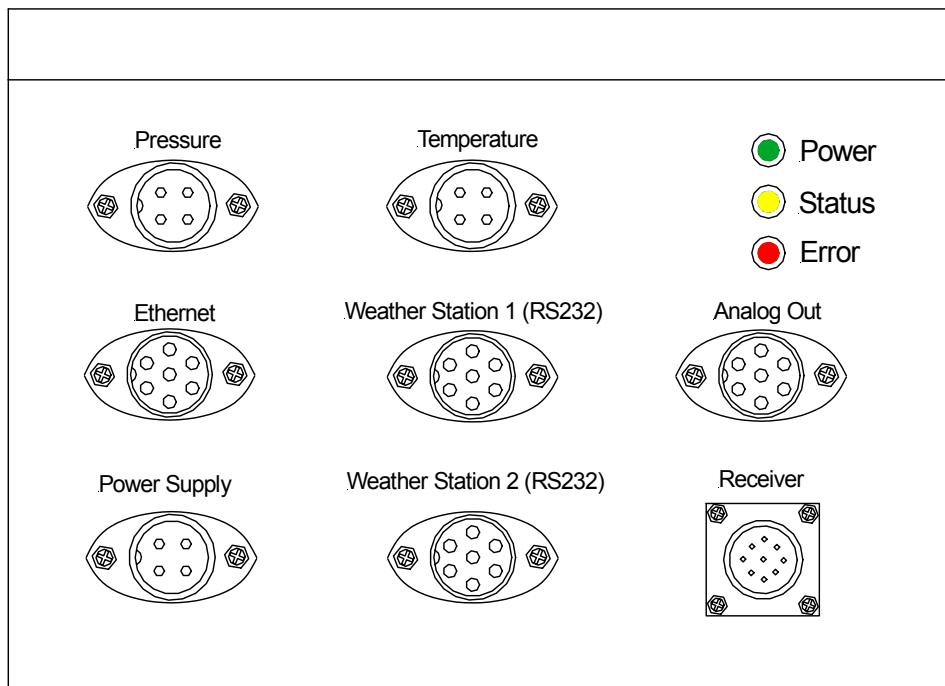


Figure 10: SPU front view

The data held in the memory of the SPU are read out by a PC via an Ethernet cable link and are finally stored as ASCII files on the internal hard disk. From the stored data the software displays in tabulated or graphical form the time series of  $C_n^2$ ,  $r_o$  and  $u$ . The pulse height statistics are equally available, and a data quality rating is given.

The software can also be used to analyse the system performance in real time, when a PC is connected to the SPU. This is particular helpful during set-up or alignment.

### 4.3.2 POWER SUPPLY

The Signal Processing Unit (SPU) generates the 12V DC voltages needed for the BLS receiver from an external power supply. For this, a single 12 V supply voltage with a peak current capability of around 2 A is required. Connection between the power source and the SPU is established via the supplied battery power supply cable having the following color code:

- red cable: supply voltage +12 V (max 13.8 V, 2 A peak)
- black cable: supply voltage ground

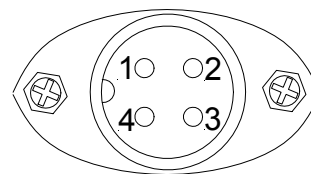
### 4.3.3 CONNECTORS

The BLS SPU is equipped with the following connectors:

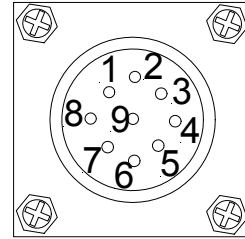
- Power Supply
- Ethernet
- Receiver
- Weather Station 1 (RS232)
- Weather Station 2 (RS232)
- Analog Out
- Pressure
- Temperature

The following table gives an overview about all pin connection schemes:

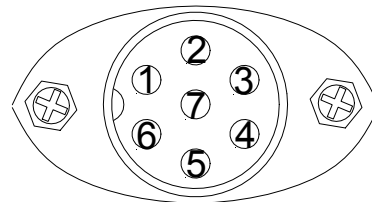
<b>Male Connector: Power Supply</b>	
<b>Function</b>	<b>Pin</b>
+12 VDC	1
+12 VDC	2
GND	3
GND	4



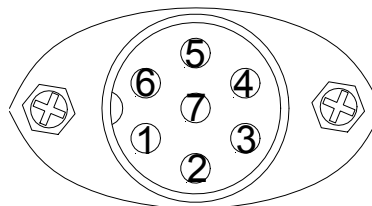
<b>Male Connector: Receiver</b>	
<b>Function</b>	<b>Pin</b>
-12V DC	1
+12V DC	2
GND	3
Signal B	4
Signal A	5
Reserved	6
Reserved	7
Reserved	8
GND	9



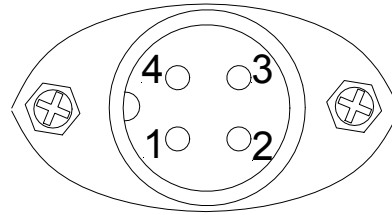
<b>Male Connector: Ethernet</b>	
<b>Function</b>	<b>Pin</b>
Signal TX-	1
Signal TX+	2
Signal RX-	3
Signal RX+	4
Not connected	5
Not connected	6
Not connected	7



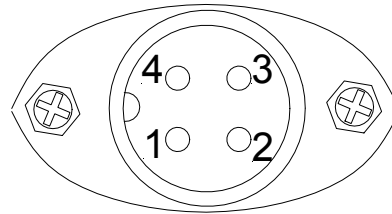
<b>Female Connectors: Weather Station 1 (RS232) Weather Station 2 (RS232)</b>	
<b>Function</b>	<b>Pin</b>
GND	1
Signal RX	2
Signal TX	3
+12V DC	4
Reserved	5
Not connected	6
GND	7



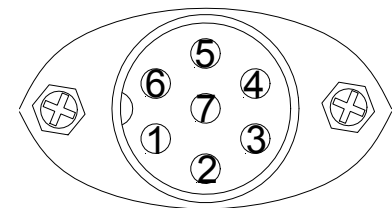
<b>Female Connector: Pressure</b>	
<b>Function</b>	<b>Pin</b>
+12V DC	1
GND	2
Signal Pressure	3
Not connected	4



<b>Female Connector: Temperature</b>	
<b>Function</b>	<b>Pin</b>
+12V DC	1
GND	2
Signal Temperature 1	3
Signal Temperature 2	4



<b>Female Connector: Analog Out</b>	
<b>Function</b>	<b>Pin</b>
GND	1
Signal XA	2
Signal YA	3
+12V DC	4
Alignment Signal XB	5
Alignment Signal YB	6
GND	7



#### 4.3.4 CURRENTS ON WEATHER STATION PORTS AND ANALOG OUT

Any devices that are connected to Weather Station Port 1, Weather Station Port 2 and Analog Out can be supplied with voltages by the SPU (see Section 4.3.3 for corresponding pin connection schemes).

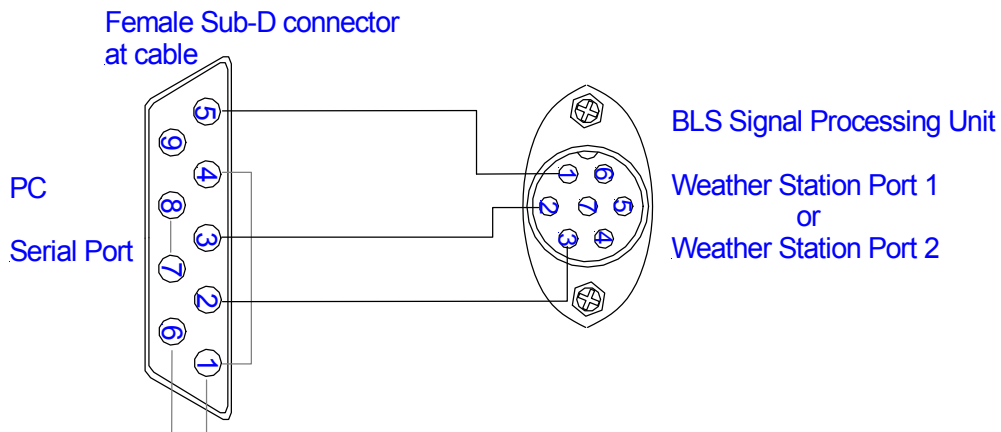
#### **IMPORTANT USER INFORMATION**

**All devices connected to Weather Station Port 1, Weather Station Port 2 and Analog Out may not draw more than 300mA in total at 12VDC provided by the SPU.**

#### 4.3.5 WEATHER STATION CABLE WITH PC CONNECTOR

This cable can be plugged into the Weather Station Port of the Signal Processing Unit. It ends with a female Sub-D connector that can be connected to the serial port of a PC or other RS232 data terminal equipment (DTE). This permits to transmit BLS measurement data in real-time over serial line. You may also utilize this cable to change the network configuration of the SPU via a PC running Hyperterminal (see the Software Manual for details).

The cable is configured as shown in the following illustration:



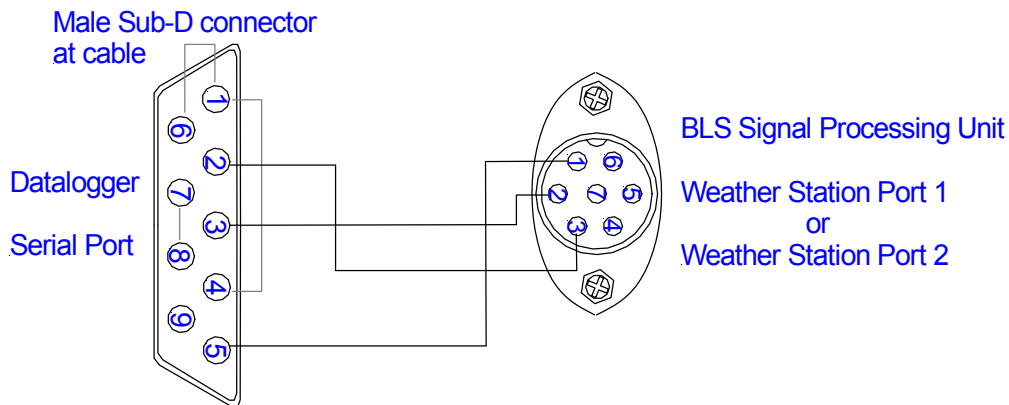
The pinout of the female Sub-D connector is given below:

Function	Sub-D Pin
Carrier Detect	1 (Connected to pin 4,6)
Signal RX	2
Signal TX	3
Data Terminal Ready	4 (Connected to pin 1,6)
GND	5
Data Set Ready	6 (Connected to pin 1,4)
Request To Send	7 (Connected to pin 8)
Clear To Send	8 (Connected to pin 7)
Ring Indicator	9 (Not connected)

### 4.3.6 WEATHER STATION CABLE WITH DATALOGGER CONNECTOR (OPTIONAL)

This optionally available cable can be plugged into the Weather Station Port of the Signal Processing Unit. It ends with a male Sub-D connector that can be directly connected to a datalogger or other RS232 data communication equipment (DCE). The cable can be used either to provide the BLS with additional meteorological sensor data – or to have the BLS measurement data transmitted in real-time to your equipment.

The cable is configured as shown in the following illustration:



The pinout of the male Sub-D connector is given below:

Function	Sub-D Pin
Carrier Detect	1 (Connected to pin 4,6)
Signal RX	2
Signal TX	3
Data Terminal Ready	4 (Connected to pin 1,6)
GND	5
Data Set Ready	6 (Connected to pin 1,4)
Request To Send	7 (Connected to pin 8)
Clear To Send	8 (Connected to pin 7)
Ring Indicator	9 (Not connected)

### 4.3.7 WEATHER STATION CABLE WITH OPEN WIRES (OPTIONAL)

This optionally available cable can be plugged into the Weather Station Port of the Signal Processing Unit. It ends with open wires that can be connected to a datalogger or other RS232 equipment. This way you may either provide the BLS with additional meteorological sensor data – or you may have the BLS measurement data transmitted in real-time to your equipment.

The color code of the open wires is given below:

Function	Color
GND	Black
Signal RX	Yellow
Signal TX	Green
+12V DC	White
Reserved	Brown
GND	Blue and Purple

---

#### 4.3.8 ANALOG OUT CABLE WITH OPEN WIRES (OPTIONAL)

The analog out cable with open wires is optionally available to connect the Analog Out Port of the Signal Processing Unit to an external datalogger or other signal processing equipment. The cable carries voltage signals between 0V and +10V that are proportional to the received light intensity in the respective measurement channels.

The color code of the open wires is given below:

<b>Function</b>	<b>Color</b>
GND	Black
Signal XA	Yellow
Signal YA	Green
+12V DC	White
Alignment Signal XB	Brown
Alignment Signal YB	Blue
GND	Purple

---

## 4.4 BLS POWER SUPPLY (OPTIONAL)

On request, the BLS system is available with additional BLS Power Supply units for the SPU and the transmitter, respectively. One BLS Power Supply comes with an attached 10 m cable for mains connection (AC In) and a second cable for establishing power support to the SPU or the transmitter (DC Out). The standard length is 3 m and 4 m to the SPU and the transmitter, respectively.

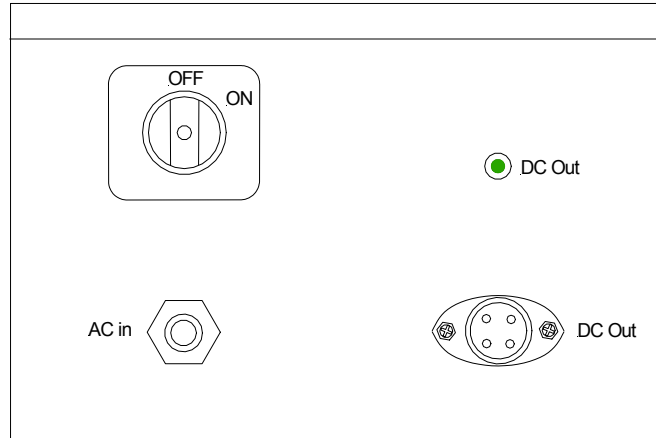


Figure 11: BLS Power Supply front view

## 4.5 BLS UNINTERRUPTIBLE POWER SUPPLY (OPTIONAL)

On request, additional BLS Uninterruptible Power Supply (UPS) units are available for the BLS Power Supply units. A BLS UPS comes with a 1 m cable (DC In) for connection to the BLS Power Supply. A BLS UPS serves as a battery backup with around 40 Ah. Based on Pulse Width Modulation (PWM), the battery is automatically recharged. The BLS UPS is also equipped with a low voltage disconnect, which disconnects the battery once the battery voltage falls below a certain threshold.

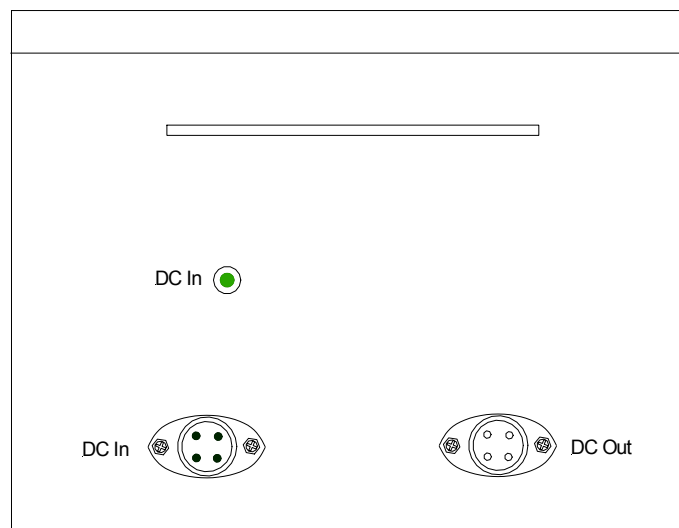


Figure 12: BLS UPS front view

---

## 4.6 DIRECT METEOROLOGICAL INPUT BLSDMI-1 (OPTIONAL)

### 4.6.1 OVERVIEW

The BLSDMI-1 option consists of a temperature sensor, a barometric pressure sensor, a small tower and cables to connect the sensors to the SPU. The sensors measure continuously air pressure and temperature and the software uses these measured parameters in real-time for the heat flux calculation.

The PT1000 temperature sensor is plugged into a ventilated radiation shield which can be installed on the tower. The radiation shield avoids measurement errors due to sun radiation. The PT1000 is connected to a BLSDMI sensor interface which converts the PT1000 resistance into a voltage. This voltage output is connected to the analogue input board of the SPU.

The barometric pressure sensor includes a voltage output which is connected directly to the SPU.

### 4.6.2 APPLIANCE

The temperature sensor can be fixed on the tower, and should be located next to the measurement range to account for accurate results. The cable between the temperature sensor interface and the SPU is 10m as standard.

The DC power for the sensor interface is supplied via cable from the SPU. The AC power for the shield aspiration must be provided next to the tower. The pressure sensor is delivered with a 5 m cable and can be fixed next to the SPU. The DC power for the pressure sensor is supplied via cable from the SPU.

The SPU includes two connectors for temperature and pressure. An electrical connection scheme of the BLSDMI-1 option is shown in the following figure:

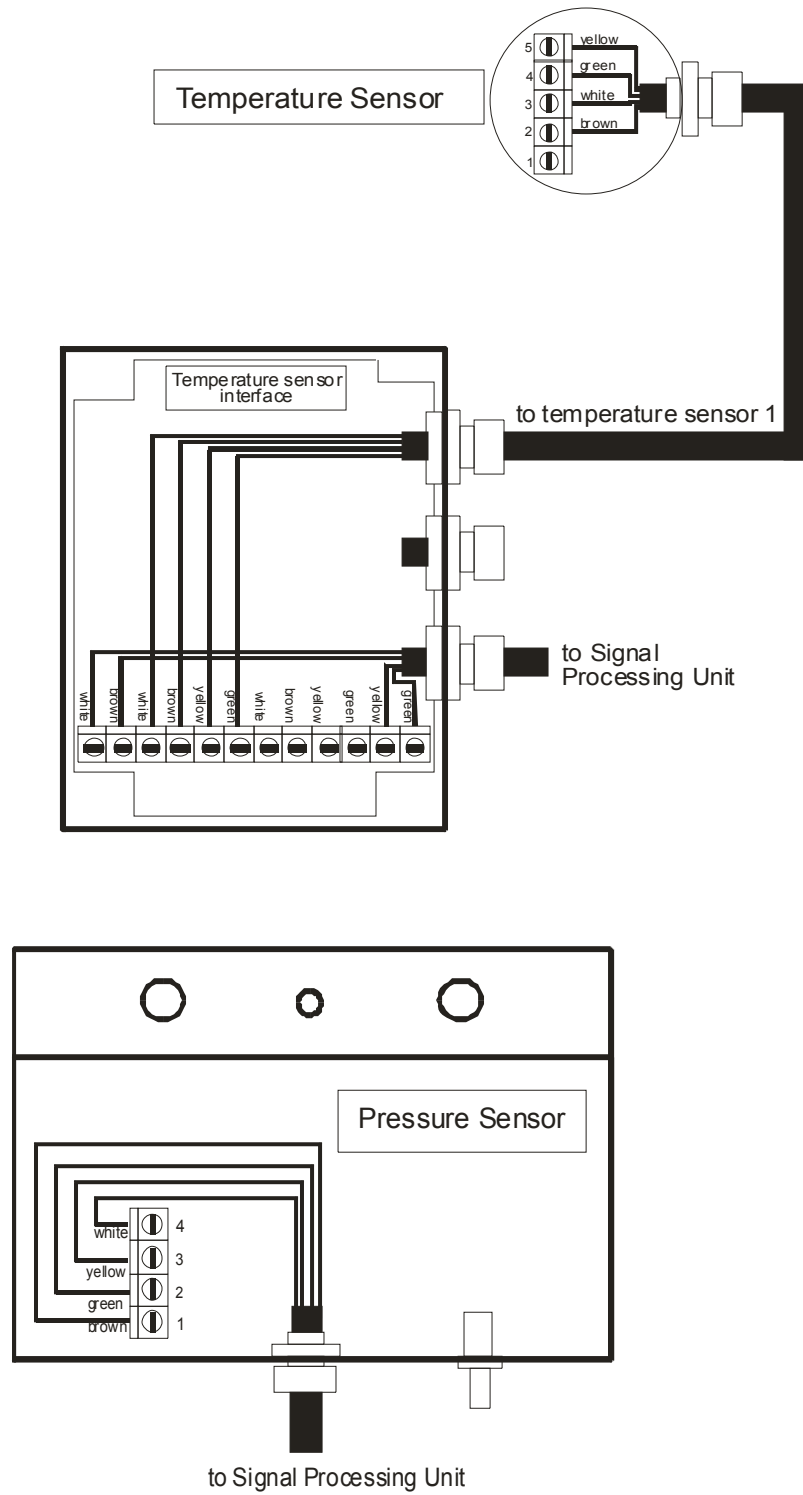
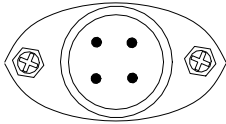


Figure 13: Electrical connections of the BLSDMI-1 sensors

## 4.7 BLS2000 RECEIVER HEATING (OPTIONAL)

On request, the BLS2000 Receiver is available with an additional heating system for the collimating Fresnel lens. The BLS SPU is then equipped with an additional connector labeled "Heating 12 VDC":



Pin #	Signal
1	+12 VDC
2	GND
3	Not Connected
4	Not Connected

Figure 14: BLS2000 Heating connector at SPU and corresponding pin signals

To operate the BLS2000 Receiver with lens heating, plug the corresponding battery power supply cable into the connector and connect the two open ends to a battery. The DC power for the lens heating is supplied via the cable connecting the SPU and the BLS2000 Receiver.

## 4.8 PATH REDUCTION APERTURE (OPTIONAL)

The optionally available path reduction aperture is a set of special disks. This set enables one to reduce the path length between the BLS Receiver and the Transmitter. By using the path reduction aperture, shorter path lengths down to 250 m and 1000 m can be realized for the BLS450/BLS900 and the BLS2000, respectively. For details on the changed measurement ranges, see Table 1.

The Path Reduction Aperture comprises 1 disk for the BLS Receiver and 1 or 2 disks for the BLS450 or BLS900/BLS2000 Transmitter, respectively. Note that the path reduction aperture disks must always be used at the transmitter and the receiver simultaneously.

### 4.8.1 RECEIVER PATH REDUCTION APERTURES

The Receiver Path Reduction Aperture is placed in front of the collimating lens of the BLS Receiver and is mechanically fixed to the BLS Receiver by three screws (

Figure 15 and

Figure 16).

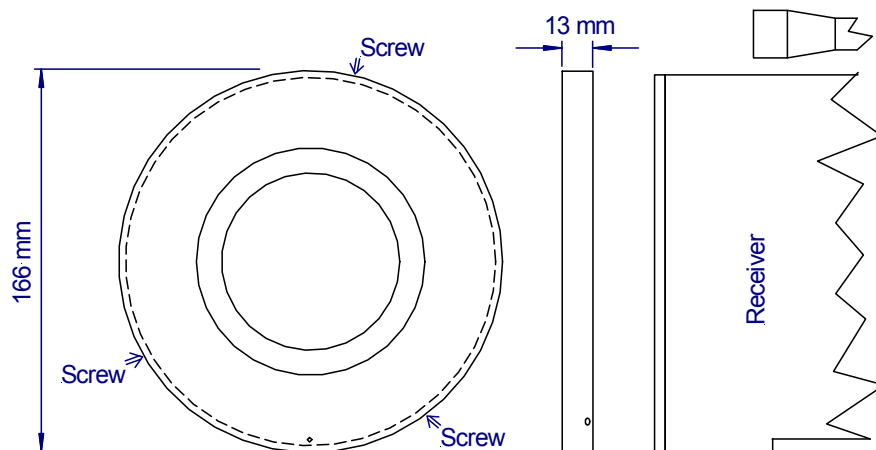


Figure 15: Receiver Path Reduction Aperture for BLS450 and BLS900

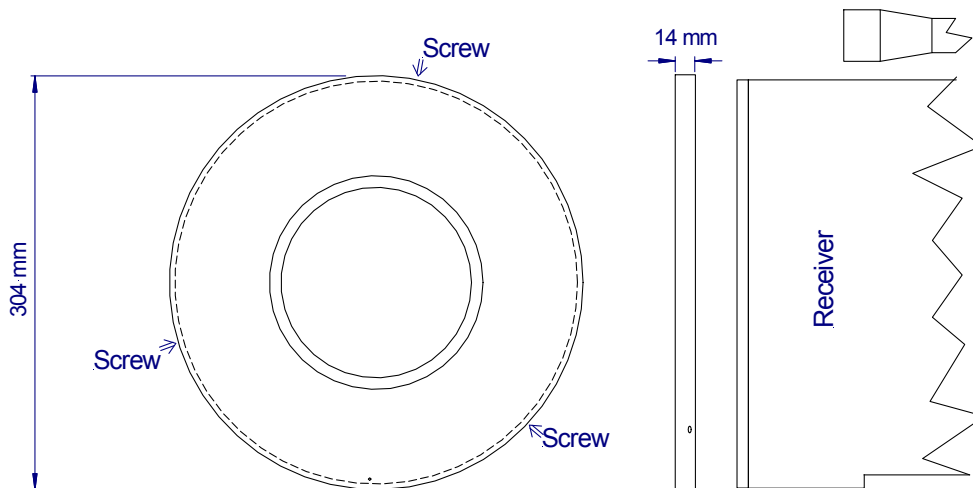


Figure 16: Receiver Path Reduction Aperture for BLS2000

#### 4.8.2 TRANSMITTER PATH REDUCTION APERTURES

The Transmitter Path Reduction Apertures are placed in front of each radiating disk of the BLS Transmitter. They are mechanically fixed to the BLS Transmitter by three screws (Figure 17 and Figure 18). The Transmitter Path Reduction Apertures disks for BLS900 and BLS2000 Transmitters are flattened at the side.

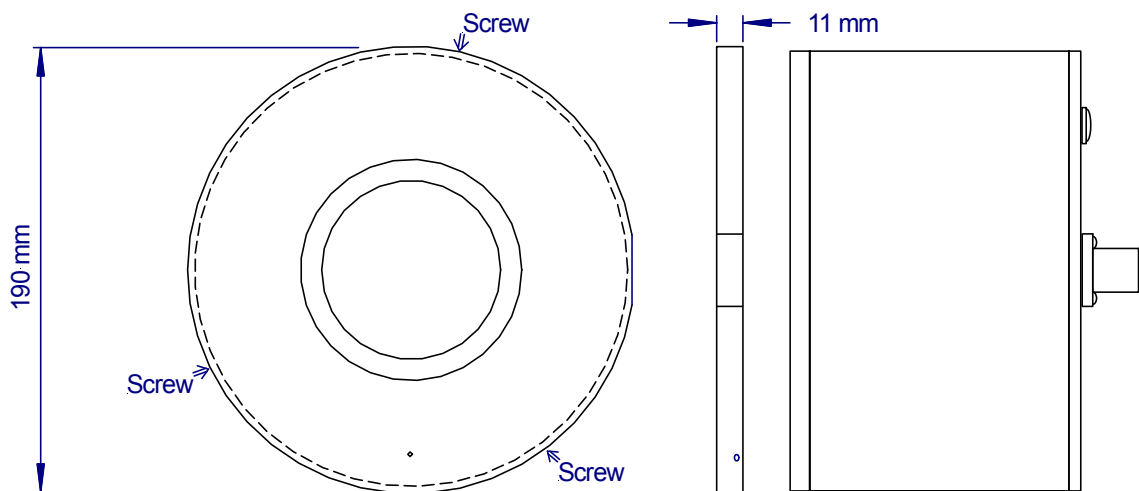


Figure 17: Transmitter Path Reduction Aperture for BLS450 and BLS900

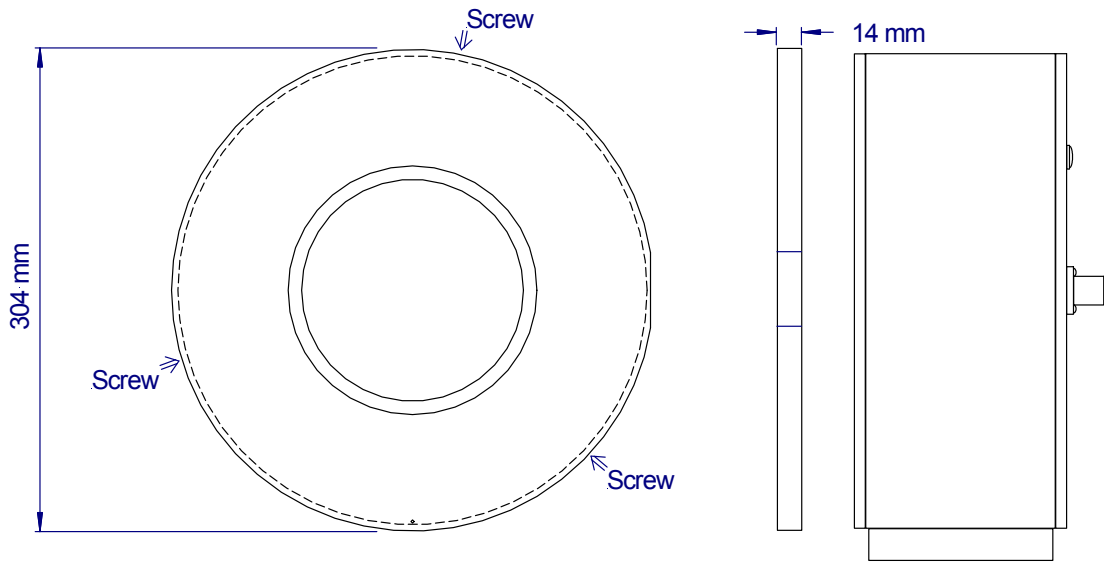


Figure 18: Transmitter Path Reduction Aperture for BLS2000

---

## APPENDIX A THEORY

### A.1 OVERVIEW

Intensity fluctuations caused by atmospheric turbulence are called "weak", when the observed log-amplitude (or intensity) variance is proportional to the refractive index structure function constant  $C_n^2$  with all other instrumental characteristics unchanged. This is also often called "weak scattering" or "weak turbulence". If proportionality is not given, the turbulent intensity fluctuations are called "strong". Intensity fluctuations transit from weak to strong with increasing  $C_n^2$  and/or increasing path length. When during this transition, the proportionality between intensity fluctuations and  $C_n^2$  is no longer observed, the phenomenon is called "saturation".

The assumption of weak turbulence facilitates the theoretical treatment. Therefore it should be used whenever possible. Physically it means that the perturbations of the phase fronts are sufficiently small to construct interference patterns simply by overlaying the distorted with the undistorted electromagnetic field.

The question whether scattering is weak or not has always to be related to the system under consideration. For the same atmospheric turbulence condition ( $C_n^2$ ), one electro-optical system may have to be treated with strong scattering theory while a second system may still be described using weak scattering theory.

Due to its large emission and reception apertures, the BLS450, BLS900 and BLS2000 are relatively insensitive to saturation. Therefore the operation can often sufficiently be described by use of weak scattering theory. This is done in section A.2. For extension into conditions of strong turbulence, see section A.3.

The theoretical description is for the BLS900 and BLS2000. For the BLS450, all calculations and algorithms involving disk 2 are not applied.

### A.2 MEASUREMENTS UNDER CONDITIONS OF WEAK SCATTERING

The BLS900 and BLS2000 measure the following statistics:

Average received intensity originating from disk 1:	$\langle I_1 \rangle$
Average received intensity originating from disk 2:	$\langle I_2 \rangle$
Variance of received intensity originating from disk 1:	$\sigma_{11}$
Variance of received intensity originating from disk 2:	$\sigma_{22}$
Covariance of rec. intensities originating from disks 1 and 2, resp.:	$\sigma_{12}$

(Note that standard deviations and correlations are output in the diagnosis files instead of variances and covariances.)

Since the theory is for log-amplitude variances  $B_{11}$ ,  $B_{22}$ , and covariances  $B_{12}$ , the above measured statistics must be converted first. This is done using the relations

$$B_{11} = \frac{1}{4} \ln \left[ 1 + \frac{\sigma_{11}}{\langle I_1 \rangle^2} \right]$$

and

$$B_{22} = \frac{1}{4} \ln \left[ 1 + \frac{\sigma_{22}}{\langle I_2 \rangle^2} \right]$$

(1)

$$B_{12} = \frac{1}{4} \ln \left[ 1 + \frac{\sigma_{12}}{\sqrt{\sigma_{11} \sigma_{22}}} \left[ \left( \frac{\sigma_{11}}{\langle I_1 \rangle^2} + 1 \right)^{\frac{1}{2}} \left( \frac{\sigma_{22}}{\langle I_2 \rangle^2} + 1 \right)^{\frac{1}{2}} - 1 \right] \right]$$

(2)

which are valid for statistics having log-normal distribution. In the above equations, it has also to be considered that the intensity is the square of the amplitude.

Weak scattering theory relates  $B_{11}$ ,  $B_{22}$  and  $B_{12}$  to the three-dimensional spectrum of the refractive index fluctuations  $\Phi_n$  [1]:

$$B_{11} = B_{22} = 4 \pi^2 k^2 \int_0^\infty d\kappa \kappa \Phi_n(\kappa) \int_0^R dx \sin^2 \left( \frac{\kappa^2 x(R-x)}{2kR} \right)$$

(3)

$$\left[ \frac{J_1 \left( \frac{\kappa D_r x}{2R} \right)}{2 \frac{\kappa D_r x}{2R}} \right]^2 \left[ \frac{J_1 \left( \frac{\kappa D_t (R-x)}{2R} \right)}{2 \frac{\kappa D_t (R-x)}{2R}} \right]^2$$

and

$$B_{12} = 4 \pi^2 k^2 \int_0^\infty d\kappa \kappa \Phi_n(\kappa) \int_0^R dx \sin^2 \left( \frac{\kappa^2 x(R-x)}{2kR} \right) J_0 \left( \kappa S_t \left( 1 - \frac{x}{R} \right) \right)$$

(4)

$$\left[ \frac{J_1 \left( \frac{\kappa D_r x}{2R} \right)}{2 \frac{\kappa D_r x}{2R}} \right]^2 \left[ \frac{J_1 \left( \frac{\kappa D_t (R-x)}{2R} \right)}{2 \frac{\kappa D_t (R-x)}{2R}} \right]^2$$

Here  $k=2\pi/\lambda$  is the wave number of the radiation,  $\kappa$  is the spatial wave number,  $x$  is the length coordinate along the propagation path and  $J_0$  and  $J_1$  denote Bessel functions of the first kind.

The three-dimensional spectrum of the refractive index fluctuations is given by the model equation

$$\Phi_n(\kappa) = 0.033 C_n^2 \kappa^{-11/3} f(\kappa \ell_0) F(\kappa L_0) \quad (5)$$

where  $f(\kappa \ell_0)$  and  $F(\kappa L_0)$  are functions describing the decay of the refractive index fluctuations at eddy sizes below the inner scale  $\ell_0$  and above the outer scale  $L_0$ , respectively.  $f$  is 1 for  $\kappa \ll 1/\ell_0$  and approaches 0 for  $\kappa \gg 1/\ell_0$ .  $F$  is 1 for  $\kappa \gg 1/L_0$  and approaches 0 for  $\kappa \ll 1/L_0$ .

Using Eqs.(3) and (4) it can be shown that the BLS900 and BLS2000 respond to refractive index eddy sizes in the order of the size of the emitting disks  $D_t = 0.15$  m and  $D_t = 0.26$  m, respectively. The inner scale is a few millimetres only, the outer scale is a few meters to a few hundred meters, depending on the meteorological conditions. Both scales are very different from  $D_t$ , hence inner and outer scale effects are negligible. This formally means that in Eq.(5), the assumptions  $f(\ell_0 \kappa) = 1$  and  $F(L_0 \kappa) = 1$  are justified for calculation purposes.

Since  $D_t$  (and  $D_r$ ) is much larger than the Fresnel zone  $(\lambda R)^{1/2}$ , the wavelength dependence also becomes negligible. Under these conditions, insertion of Eq.(5) into Eq.(3) and integration leads to the following approximate expression (Ting-i Wang et al., 1978):

$$C_n^2 = \alpha_r B_{11} D_t^{7/3} R^{-3} = \alpha_r B_{22} D_t^{7/3} R^{-3} \quad (6)$$

The factor  $\alpha_r$  depends on the ratio of the transmitting to the receiving aperture. For the BLS900  $\alpha_r = 4.629$ , for the BLS2000  $\alpha_r = 4.49$ .

The relationship between the variances and the third power of the path length  $R^3$  is shown in Figure 19 for the BLS900 and for  $C_n^2 = 10^{-12} \text{ m}^{-2/3}$ . The solid line is plotted using equation (6), the symbols are calculated using equation (3).

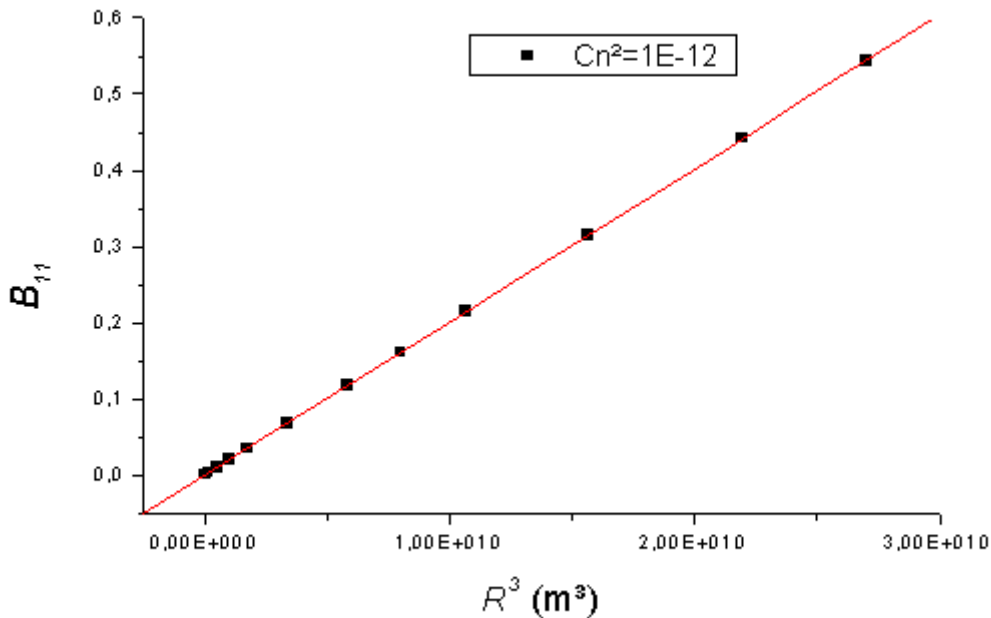


Figure 19: Relation between the log-amplitude B11 and the path length R3 for the BLS900

### A.3 MEASUREMENTS UNDER CONDITIONS OF STRONG SCATTERING

After propagation through sufficiently strong integrated turbulence, the coherence of the phase fronts is reduced such that the theory given in section A.2 requires modification. In order to describe the resulting effect of saturation of scintillation, Clifford et al. [2] suggest that a short term MTF

$$M_{ST}(y, x) = \exp(-0.05 \pi^2 k^2 C_n^2 x y^{5/3} \int_{0.35ky}^{\infty} d\xi \xi^{8/3} [1 - J_0(\xi)]) \quad (7)$$

has to be applied during numerical integration, where the length coordinate  $y$  perpendicular to the propagation direction has to be substituted by  $\kappa x(1 - x/R)/k$ .

Accordingly, the log-amplitude variances and covariances which include the effect of saturation are

$$B_{11} = B_{22} = 4 \pi^2 k^2 \int_0^{\infty} d\kappa \kappa \Phi_n(\kappa) \int_0^R dx \sin^2\left(\frac{k^2 x(R-x)}{2kR}\right) \quad (8)$$

$$M_{ST}\left(\kappa x\left(1 - \frac{x}{R}\right)/k, R\right) \left[ 2 \frac{J_1\left(\frac{\kappa D_r x}{2R}\right)}{\frac{\kappa D_r x}{2R}} \right]^2 \left[ 2 \frac{J_1\left(\frac{\kappa D_t(R-x)}{2R}\right)}{\frac{\kappa D_t(R-x)}{2R}} \right]^2$$

and

$$B_{12} = 4 \pi^2 k^2 \int_0^{\infty} d\kappa \kappa \Phi_n(\kappa) \int_0^R dx \sin^2\left(\frac{k^2 x(R-x)}{2kR}\right) J_0\left(\kappa S_t\left(1 - \frac{x}{R}\right)\right) \quad (9)$$

$$M_{ST}\left(\kappa x\left(1 - \frac{x}{R}\right)/k, R\right) \left[ 2 \frac{J_1\left(\frac{\kappa D_r x}{2R}\right)}{\frac{\kappa D_r x}{2R}} \right]^2 \left[ 2 \frac{J_1\left(\frac{\kappa D_t(R-x)}{2R}\right)}{\frac{\kappa D_t(R-x)}{2R}} \right]^2$$

In Figure 20,  $B_{11}$  according to equation (3) is plotted against  $B_{11}$  according to equation (8) for path lengths of 1000 m, 2000 m and 3000 m and different values of  $C_n^2$ . The effect of saturation is clearly visible: values of  $B_{11}$  do not increase so quickly with  $C_n^2$  when the strong scattering effect is taken into account. It can also be seen that the magnitude of the effect differs with the propagation path length.

The BLS900 and the BLS2000 use a numerical look-up table to correct for the effect of saturation. In this look-up table, also a maximum value for  $(B_{11} + B_{22})/2$  is defined. If a larger value is measured, an unambiguous determination of  $C_n^2$  is impossible and an error message is output by the instrument.

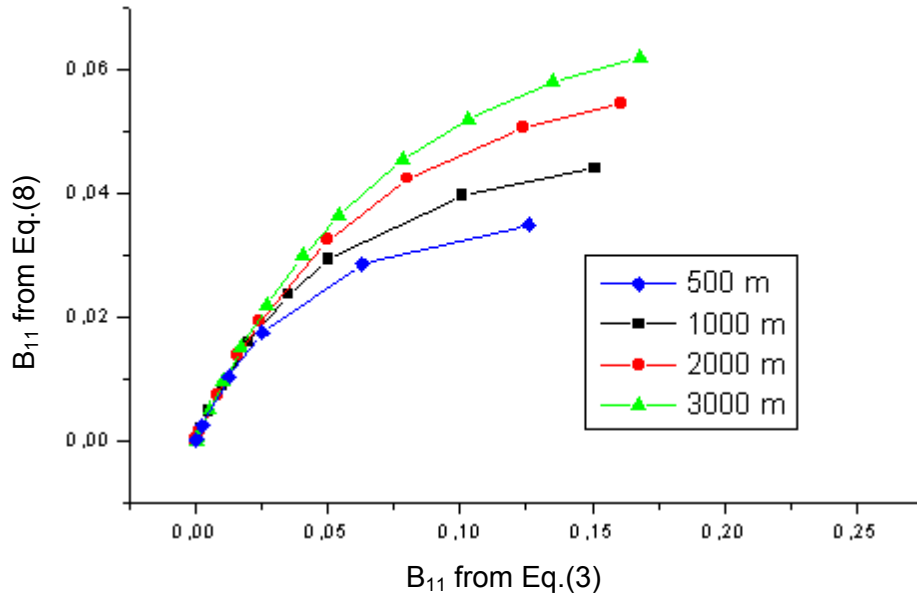


Figure 20: Comparison of log-amplitude variances  $B_{11}$  including and excluding saturation

## A.4 ABSORPTION FLUCTUATIONS

For weak turbulence, the BLS900 and the BLS2000 evaluate the quantity  $Q = (B_{11} + B_{22})/2 - B_{12}$  instead of the variances  $B_{11}$  and  $B_{22}$  or the average variance  $(B_{11} + B_{22})/2$ . The advantage of using  $Q$  compared to using the variances  $B_{11}$  or  $B_{22}$  is that  $Q$  is not affected by absorption fluctuations. The expression "absorption fluctuations" means changes of the received intensity due to changes of the transmission over the propagation path for example due to dust or fog. This is different from changes of the received intensity due to scintillation which is caused by interference (focusing and defocusing) at temperature inhomogeneities with unchanged transmission. If not distinguished, however, absorption fluctuations may be falsely interpreted as scintillation, hence causing erroneous results.

Because absorption fluctuations are caused by inhomogeneities which have a spatial scale in the order of the path length, the changes of the intensity due to absorption will be nearly identical and highly correlated over the two paths (the paths leading to  $B_{11}$  and  $B_{22}$ ). Therefore the magnitude of absorption fluctuations contributing to  $B_{11}$ ,  $B_{22}$  and  $B_{12}$  is nearly identical, and absorption fluctuations are widely eliminated by subtracting  $B_{12}$  from  $(B_{11} + B_{22})/2$  in  $Q$ .

Temperature (and refractive index) inhomogeneities causing scintillation, on the other hand, have a spatial scale which is in the order of the size of the radiating disks (in general: size of emitting aperture or size of receiving aperture, whichever is larger). Since the separation between the disks is larger than the disk size, the covariance  $B_{12}$  is much smaller than the variances. Fig.16 shows the relation between  $Q$  and  $R^3$ , again for  $C_n^2 = 10^{-12} \text{ m}^{-2/3}$ . The symbols were calculated using Eqs.(3) and (4). The line is a good approximation. The ratio of the covariances to the variances can be calculated to be  $B_{12} / B_{11} = 0.106$  for the BLS900 and  $B_{12} / B_{11} = 0.127$  for the BLS2000 independent of path length.

For measured log-amplitude variances above 0.02, the evaluation is no longer based on the quantity  $Q$  but on the quantity  $(B_{11}+B_{22})/2$ . This separation is made because the effect of saturation is less pronounced for  $B_{11}$  than for  $Q$  and also because the relative contribution of absorption fluctuations is smaller when there is stronger turbulence.

In Figure 21 the relation between  $Q$  and the path length  $R^3$  is plotted for  $C_n^2 = 10^{-12}$ . The straight line is calculated using equation 6 with  $B_{12} / B_{11} = 0.106$ , the dots are calculations using equations (3) and (4). Saturation effects are not included.

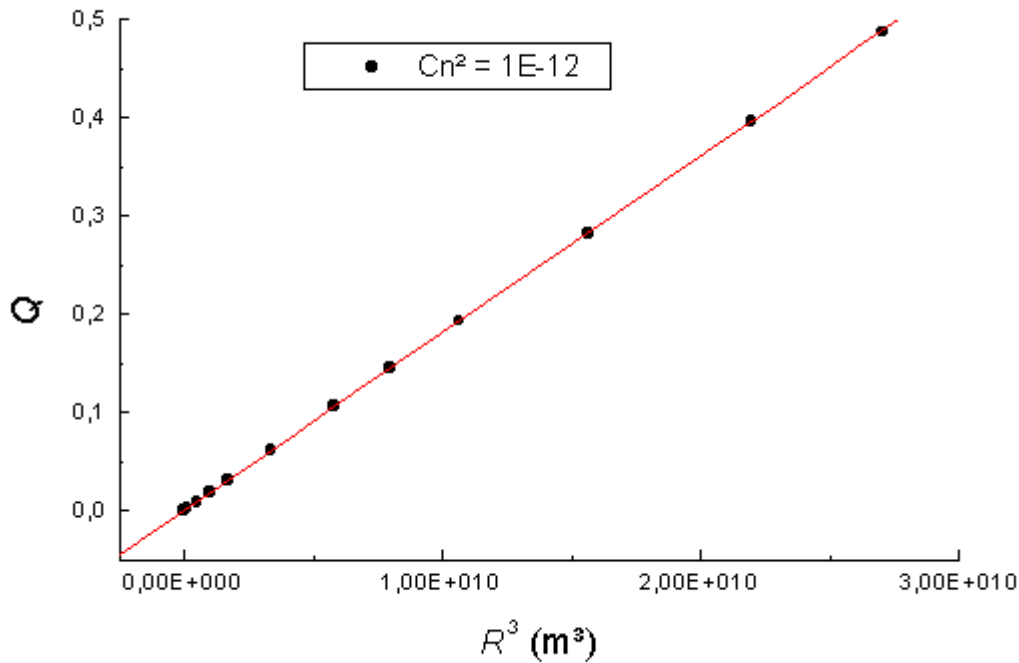


Figure 21: Relation between  $Q$  and the path length  $R^3$  for the BLS900

## A.5 WEIGHTING FUNCTIONS

Integrals like Eq.(3) can be written in the form

$$B_{11} = \int_0^{\infty} d\kappa \text{ SWF}(\kappa) \quad (10)$$

or

$$B_{11} = \int_0^R dx \text{ PWF}(x) \quad (11)$$

$\text{SWF}(\kappa)$  is the spectral weighting function describing the contribution of different regions of the refractive index spectrum (as a function of spatial wave number  $\kappa$ ) to the measured statistics, here  $B_{11}$ . Figure 22 and Figure 23 show the normalized spectral weighing function  $\kappa\text{SWF}(\kappa)$  for the variance  $B_{11}$  and  $Q$  at a path length of 1000 m. Tabular values are presented in the next section.  $Q$  is less sensitive to smaller spatial wave numbers between  $1\text{m}^{-1}$  and  $10\text{m}^{-1}$  than  $B_{11}$  while the weighting functions around the peak value around  $\kappa = 40\text{m}^{-1}$  are nearly identical. Absorption fluctuations (see section A.4) are therefore widely eliminated.

Because the diameters of the transmitting and receiving apertures,  $D_t$  and  $D_r$ , are larger than the fresnel zone  $(\lambda R)^{1/2}$ , the weighting functions for different path lengths are nearly identical.

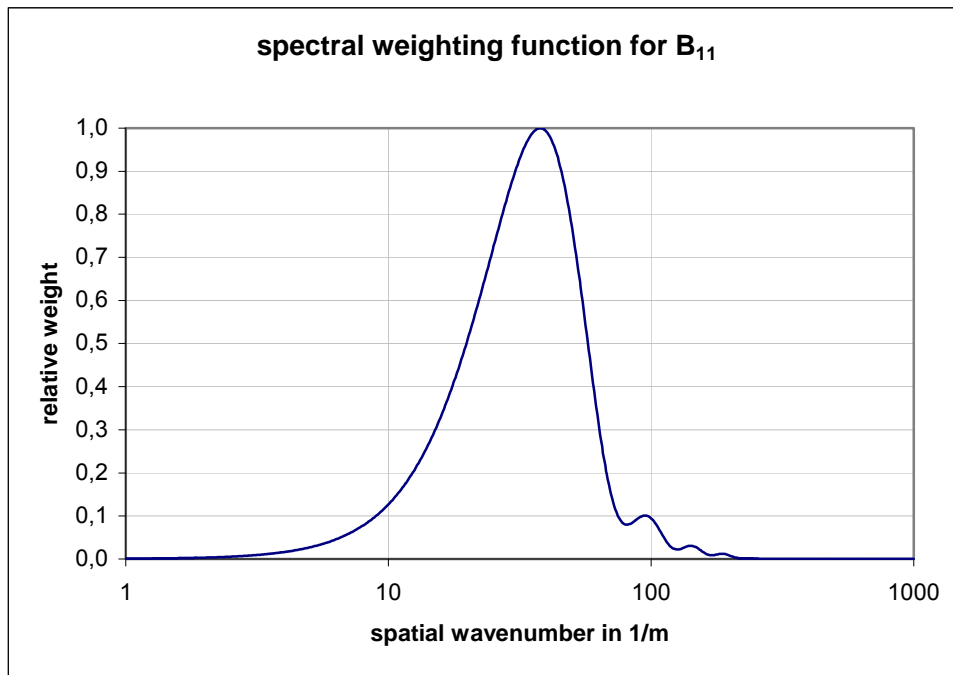


Figure 22: Spectral weighting function for  $B_{11}$ , path length is 1000m

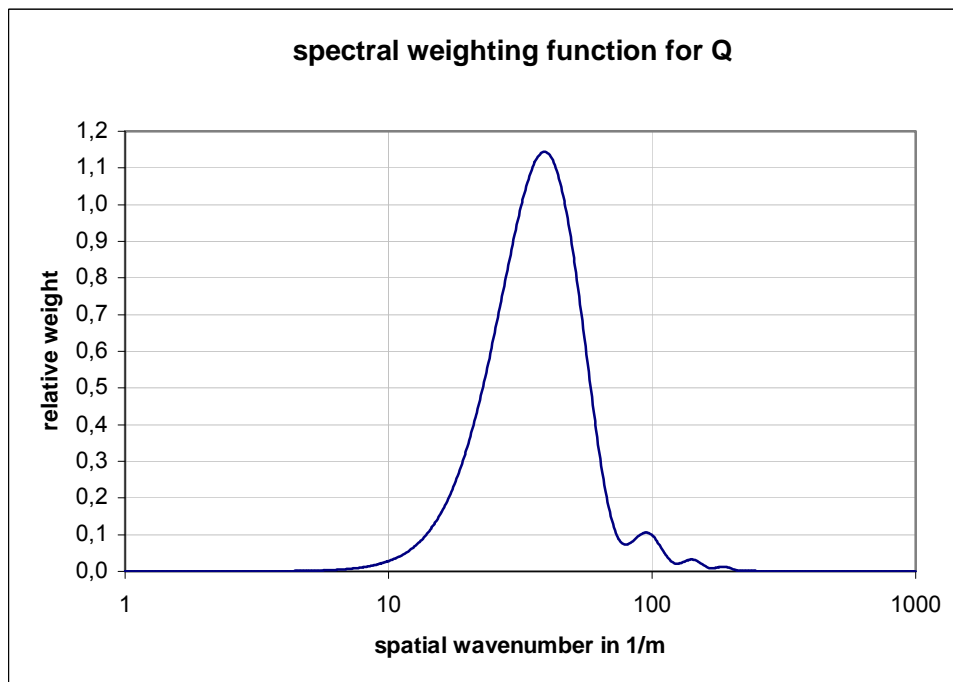


Figure 23: Spectral weighting function for  $Q$ , path length is 1000m

Accordingly,  $PWF(\kappa)$  is the spatial weighting function describing the contribution of different regions of the propagation path (as a function of path coordinate  $x$ ). The path weighting functions for  $B_{11}$  and  $Q$  as well as path weighting functions for different path lengths are quite similar and peak in the paths centre (Figure 24 and Figure 25). Tabular values and an analytic approximation are presented in later sections. The contributions of fluctuations next to the instruments are negligible leading to virtually no flow distortion by the instruments.

For heat flux calculations, in the case of uneven ground, the height of the instruments must be corrected by using the spatial weighting function. As the BLS900 / BLS2000 is most sensitive to fluctuations at the centre of the path it should be selected to be as homogenous and even as possible.

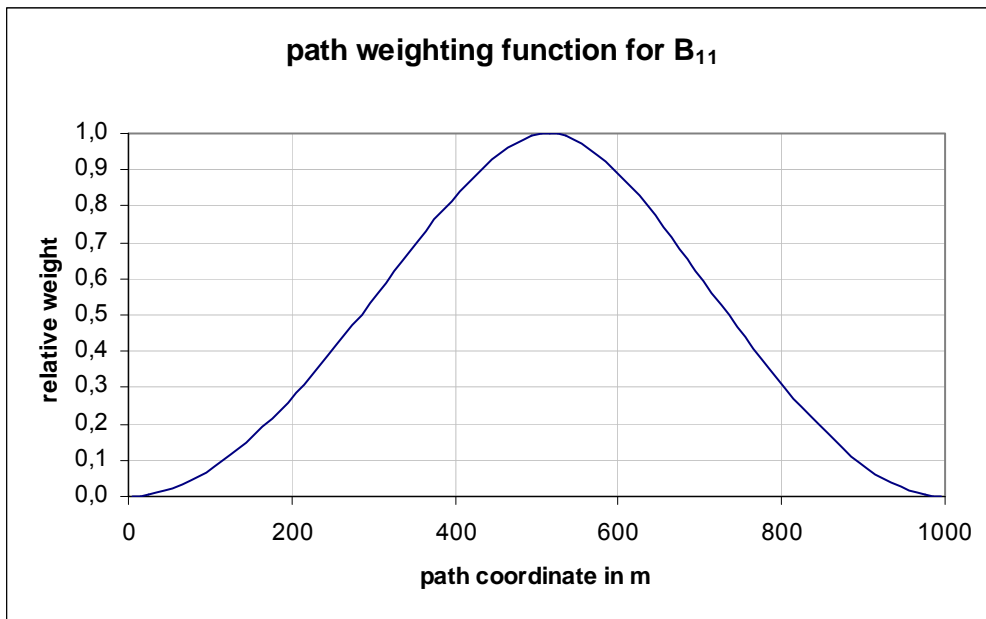


Figure 24: Spatial weighting function for B11, path length is 1000m

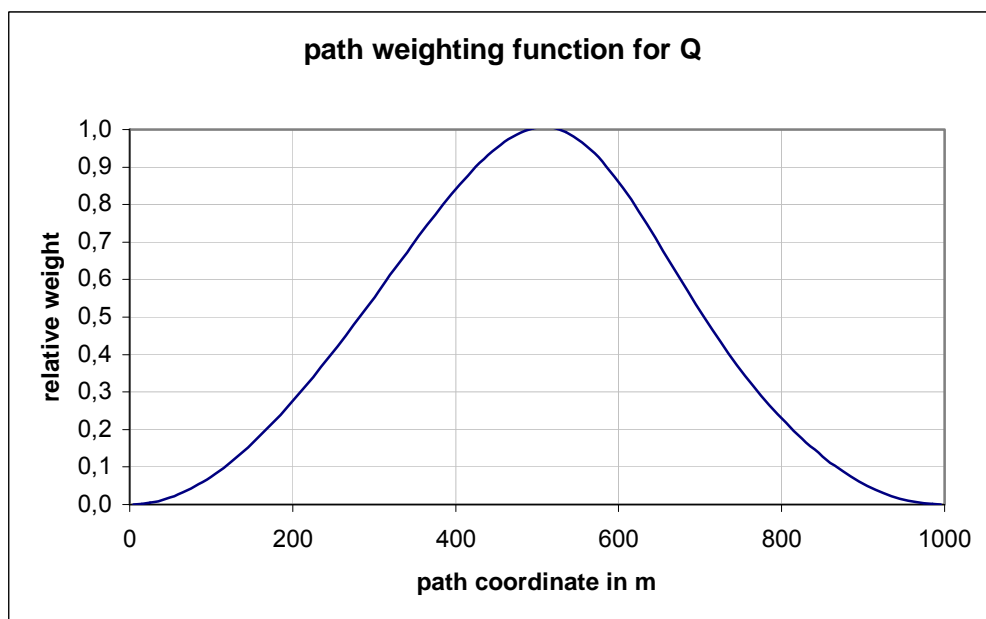


Figure 25: Spatial weighting function for Q, path length is 1000m

## A.5.1 TABULAR VALUES OF SPECTRAL WEIGHTING FUNCTION

Wavenumber	Weight for B <sub>11</sub>	Weight for Q	Wavenumber	Weight for B <sub>11</sub>	Weight for Q
0,109	0,000	0,000	10,915	0,153	0,091
0,119	0,000	0,000	11,970	0,187	0,115
0,131	0,000	0,000	13,126	0,227	0,146
0,143	0,000	0,000	14,393	0,273	0,185
0,157	0,000	0,000	15,783	0,328	0,234
0,172	0,000	0,000	17,308	0,392	0,295
0,189	0,000	0,000	18,979	0,464	0,369
0,207	0,000	0,000	20,812	0,544	0,458
0,227	0,000	0,000	22,822	0,630	0,560
0,249	0,000	0,000	25,026	0,720	0,674
0,273	0,000	0,000	27,443	0,810	0,792
0,300	0,000	0,000	30,094	0,892	0,907
0,328	0,000	0,000	33,000	0,957	1,003
0,360	0,000	0,000	36,188	0,995	1,065
0,395	0,000	0,000	39,682	0,994	1,076
0,433	0,000	0,000	43,515	0,944	1,026
0,475	0,000	0,000	47,718	0,841	0,909
0,521	0,000	0,000	52,326	0,688	0,734
0,571	0,000	0,000	57,380	0,503	0,526
0,626	0,000	0,000	62,921	0,319	0,323
0,687	0,000	0,000	68,998	0,173	0,167
0,753	0,000	0,000	75,662	0,094	0,088
0,826	0,000	0,000	82,970	0,081	0,079
0,906	0,001	0,000	90,983	0,098	0,100
0,993	0,001	0,000	99,770	0,095	0,097
1,089	0,001	0,000	109,406	0,060	0,059
1,194	0,001	0,000	119,972	0,026	0,025
1,310	0,001	0,001	131,559	0,025	0,025
1,436	0,001	0,001	144,264	0,030	0,031
1,575	0,002	0,001	158,197	0,015	0,015
1,727	0,002	0,001	173,476	0,009	0,009
1,894	0,003	0,001	190,230	0,012	0,012
2,076	0,003	0,002	208,602	0,003	0,003
2,277	0,004	0,002	228,749	0,002	0,002
2,497	0,005	0,002	250,842	0,001	0,001
2,738	0,007	0,003	275,068	0,000	0,000
3,002	0,008	0,004	301,633	0,000	0,000
3,292	0,010	0,005	330,765	0,000	0,000
3,610	0,013	0,006	362,710	0,000	0,000
3,959	0,016	0,007	397,740	0,000	0,000
4,341	0,019	0,009	436,154	0,000	0,000
4,761	0,024	0,011	478,277	0,000	0,000
5,221	0,030	0,014	524,469	0,000	0,000
5,725	0,036	0,018	575,122	0,000	0,000
6,278	0,045	0,022	630,667	0,000	0,000
6,884	0,055	0,028	691,576	0,000	0,000
7,549	0,068	0,035	758,368	0,000	0,000
8,278	0,084	0,045	831,610	0,000	0,000
9,077	0,103	0,056	911,927	0,000	0,000
9,954	0,126	0,071	1000,000	0,000	0,000

Table 4: Tabular values of spectral weighting function.

## A.5.2 TABULAR VALUES OF PATH WEIGHTING FUNCTION

Path Position	Weight for B <sub>11</sub>	Weight for Q	Path Position	Weight for B <sub>11</sub>	Weight for Q
0,5%	0,000	0,000	50,5%	0,999	1,000
1,5%	0,002	0,002	51,5%	1,000	0,999
2,5%	0,005	0,005	52,5%	0,998	0,995
3,5%	0,009	0,009	53,5%	0,993	0,987
4,5%	0,015	0,015	54,5%	0,984	0,975
5,5%	0,022	0,023	55,5%	0,972	0,960
6,5%	0,031	0,031	56,5%	0,958	0,941
7,5%	0,042	0,042	57,5%	0,941	0,920
8,5%	0,053	0,054	58,5%	0,921	0,895
9,5%	0,067	0,067	59,5%	0,900	0,869
10,5%	0,081	0,081	60,5%	0,877	0,840
11,5%	0,097	0,097	61,5%	0,853	0,809
12,5%	0,113	0,114	62,5%	0,827	0,776
13,5%	0,131	0,132	63,5%	0,800	0,742
14,5%	0,151	0,151	64,5%	0,772	0,707
15,5%	0,171	0,171	65,5%	0,743	0,672
16,5%	0,192	0,193	66,5%	0,714	0,636
17,5%	0,214	0,215	67,5%	0,684	0,600
18,5%	0,236	0,238	68,5%	0,653	0,565
19,5%	0,260	0,262	69,5%	0,623	0,530
20,5%	0,284	0,286	70,5%	0,592	0,496
21,5%	0,310	0,311	71,5%	0,561	0,463
22,5%	0,335	0,337	72,5%	0,530	0,431
23,5%	0,362	0,364	73,5%	0,499	0,400
24,5%	0,389	0,391	74,5%	0,469	0,370
25,5%	0,416	0,419	75,5%	0,439	0,342
26,5%	0,444	0,448	76,5%	0,409	0,314
27,5%	0,473	0,476	77,5%	0,380	0,288
28,5%	0,501	0,505	78,5%	0,351	0,263
29,5%	0,530	0,535	79,5%	0,324	0,239
30,5%	0,560	0,565	80,5%	0,296	0,216
31,5%	0,589	0,594	81,5%	0,270	0,195
32,5%	0,618	0,624	82,5%	0,245	0,174
33,5%	0,648	0,654	83,5%	0,220	0,155
34,5%	0,676	0,683	84,5%	0,196	0,137
35,5%	0,705	0,712	85,5%	0,174	0,119
36,5%	0,733	0,741	86,5%	0,152	0,103
37,5%	0,761	0,769	87,5%	0,132	0,088
38,5%	0,788	0,796	88,5%	0,112	0,074
39,5%	0,814	0,822	89,5%	0,094	0,061
40,5%	0,840	0,848	90,5%	0,078	0,050
41,5%	0,864	0,872	91,5%	0,063	0,039
42,5%	0,887	0,895	92,5%	0,049	0,030
43,5%	0,908	0,916	93,5%	0,037	0,022
44,5%	0,928	0,935	94,5%	0,026	0,016
45,5%	0,946	0,953	95,5%	0,018	0,010
46,5%	0,962	0,968	96,5%	0,011	0,006
47,5%	0,975	0,981	97,5%	0,005	0,003
48,5%	0,986	0,990	98,5%	0,002	0,001
49,5%	0,994	0,997	99,5%	0,000	0,000

Table 5: Tabular values of path weighting function.

---

### A.5.3 ANALYTIC APPROXIMATION OF PATH WEIGHTING FUNCTION

The path weighting function for the BLS can be analytically approximated by the following expression (by Henk de Bruin, October 2008):

$$PWF_{approx}(x) = 2.163 \cdot JJ_1(2.283 \cdot \pi \cdot (x - 0.5))$$

where  $x$  is the relative path position in the range  $0 \leq x \leq 1$  and the function  $JJ_1$  is defined as follows:

$$JJ_1(y) = \begin{cases} 1 & \text{if } y = 0 \\ \left(2 \cdot \frac{J_1(y)}{y}\right)^2 & \text{otherwise} \end{cases}$$

$J_1$  denotes the first order Bessel function of the first kind.

## A.6 RELATION TO OTHER TURBULENCE STATISTICS

Even though derived from large aperture scintillation, measurements of  $C_n^2$  obtained from the BLS900 / BLS2000 can be used to predict other turbulence statistics. A selection of corresponding formulae is given in this section [3]:

Scintillation at point detector, plane wave,  $C_n^2$  constant over path length:

$$B_{11} = 0.31 C_n^2 k^{7/6} L^{11/6} \quad (12)$$

Scintillation at point detector, plane wave,  $C_n^2$  varying over path length:

$$B_{11} = 0.56 k^{7/6} \int_0^R C_n^2(x) (R-x)^{5/6} dx \quad (13)$$

Scintillation at point detector, spherical wave (point source),  $C_n^2$  constant over path length:

$$B_{11} = 0.125 C_n^2 k^{7/6} L^{11/6} \quad (14)$$

Scintillation at point detector, spherical wave (point source),  $C_n^2$  varying over path length:

$$B_{11} = 0.56 k^{7/6} \int_0^R C_n^2(x) (x/R)^{5/6} (R-x)^{5/6} dx \quad (15)$$

Equations (12), (13), (14) and (15) are valid as long as  $l_0 \ll (\lambda R)^{1/2}$  and  $B_{11} < 0.3$  (weak scattering).

Structure function of phase between two locations separated by  $\rho$ , plane wave,  $C_n^2$  constant over path length:

$$D_p(\rho) = 2.92 C_n^2 k^2 L \rho^{5/3} \quad (16)$$

Structure function of phase for two locations separated by  $\rho$ , spherical wave,  $C_n^2$  constant over path length:

$$D_p(\rho) = (1.089 k^2 L \rho^{5/3} - 0.25 k^{7/6} L^{11/6}) C_n^2 \quad (17)$$

Equations (16) and (17) are valid as long as  $l_0 \ll (\lambda R)^{1/2}$  and  $\rho \gg (\lambda R)^{1/2}$ . Note that absolute phase fluctuations cannot be evaluated due to the dominating influence of the outer scale  $L_0$ .

$$\sigma_\alpha^2 = \frac{D_p(b)}{k^2 b^2} \quad (18)$$

With good approximation, angle-of-arrival fluctuations  $\sigma_\alpha^2$  can be calculated from the structure function of phase by setting the diameter  $b$  of the receiving telescope equal to the separation  $\rho$ :

Laser beam wander can be treated as angle-of-arrival fluctuations in reverse configuration.

For constant  $C_n^2$ , the Fried diameter  $r_0$  at the wavelength  $\lambda_0 = 2\pi/k_0$  and over the path length  $R_0$  can be calculated via the relation [4]:

$$r_0 = \left[ 0.423 k_0^2 R_0 C_n^2 \right]^{\frac{3}{5}} \quad (19)$$

## A.7 MEASUREMENT OF WIND SPEED

The transverse wind speed  $u$  is derived by an evaluation of the time lagged cross-covariance function  $B_{12}(t)$ :

$$B_{12}(t) = 4 \pi k^2 \int_0^\infty d\kappa \Phi_n(\kappa) \int_0^R dx \sin^2 \left( \frac{k^2 x(R-x)}{2kR} \right) \quad (20)$$

$$J_0 \left( \kappa (S_t - ut) \left( 1 - \frac{x}{R} \right) \right) \left[ 2 \frac{J_1 \left( \frac{\kappa D_r x}{2R} \right)}{\frac{\kappa D_r x}{2R}} \right]^2 \left[ 2 \frac{J_1 \left( \frac{\kappa D_t (R-x)}{2R} \right)}{\frac{\kappa D_t (R-x)}{2R}} \right]^2$$

A stepwise numerical de-convolution technique is applied to provide accurate results even for transverse wind speeds that vary over the propagation path and temporally fluctuate within the averaging period, including changes of sign

## A.8 MEASUREMENT OF HEAT FLUX

The calculation of the surface heat flux is based on the application of the unstable limit ( $\xi = z/L \rightarrow \infty$ ) of Monin-Obukhov similarity (free convection scaling). Here the stress becomes insignificant and the surface stress ceases to be a scaling parameter. Under these conditions the kinematic surface heat flux  $Q_0$  [unit K m/s] is

$$Q_0 = 1.165 K z C_T^{\frac{3}{4}} \left( \frac{g}{T} \right)^{\frac{1}{2}} \quad (21)$$

where  $K = 0.4$  is von Kármán's constant,  $z$  is the height above ground,  $C_T^2$  is the structure function constant of temperature fluctuations,  $g$  is gravitational acceleration and  $T$  is the air temperature. The dynamic surface heat flux  $H_0$  [unit W/m<sup>2</sup>] can be calculated by multiplication of this quantity with the density of air (1.225 kg/m<sup>3</sup> at standard temperature and pressure) and the heat capacity of air at constant pressure  $c_p$  (1004 J/kgK).

$C_T^2$  can be calculated using

$$C_n^2 = \alpha_1^2 \frac{p^2}{T^4} C_T^2 \quad (22)$$

In this formula,  $p$  is the air pressure,  $T$  is the air temperature and  $\alpha_1$  is wavelength dependant proportionality factor:

$$\alpha_1 = \alpha_2 \left( 1 + \frac{\lambda_0^2}{\lambda^2} \right) \quad (23)$$

with  $\alpha_2 = 77.6 \times 10^{-6}$  K/hPa,  $\lambda$  is the wavelength of the radiation passing through the atmosphere in  $\mu\text{m}$ , and  $\lambda_0^2 = 7.53 \times 10^{-3} \mu\text{m}^2$ .

With application of equation (22) the humidity contribution to  $C_n^2$  is neglected, which is one order of magnitude smaller than the temperature contribution. There are situations, however, especially over water, where the contribution of  $C_T^2$  is small and the humidity effect is larger.

On non-even paths the change of  $C_T^2$  must be taken into account. As  $C_T^2 \sim z^{-4/3}$ , the contribution of the temperature fluctuations is smaller with higher heights. In this case an effective height  $z_{\text{eff}}$  instead of  $z$  is calculated and equation (21) can be rewritten to

$$Q_0 = 1.165 K z_{\text{eff}} C_T^{2\frac{3}{4}} \left(\frac{g}{T}\right)^{\frac{1}{2}} \quad (24)$$

with

$$z_{\text{eff}} = \left( \int_0^1 z(x)^{-\frac{4}{3}} \cdot PWF(x) dx \right)^{-\frac{3}{4}} \quad (25)$$

where  $PWF(x)$  is the path weighting function for the BLS, which is described in a previous section, and  $z(x)$  gives the actual path height at relative path position  $0 \leq x \leq 1$ .

For slant paths, where  $z_T$  is the height of the transmitter and  $z_R$  is the height of the receiver, the path height function is given by

$$z(x) = z_T + x \cdot (z_R - z_T) \quad (26)$$

Heat flux measurements over very rough surfaces are influenced by the ground surface as well as by individual roughness elements. The reference ground (zero-plane displacement) for the height of the receiver and transmitter should therefore lie somewhere between the actual ground level and the tops of the roughness elements.

## A.9 REFERENCES

- [1] Ochs, G.R., S.F. Clifford and Ting-I Wang, Appl. Opt., 15, 403 (1976)
- [2] Clifford, S.F., G.R. Ochs and R.S: Lawrence, J. Opt. Soc. Am., 64(2), 148 (1974)
- [3] Lawrence, R.S., and J.W. Strohbehm, Proc. Of the IEEE, 58(10), 1523 (1970)
- [4] Rousset, G., Wave Propagation in Random Media (Scintillation), SPIE Bellingham & IOP Bristol, 216 (1993)
- [5] De Bruin, H., Private communication (2008)

---

## APPENDIX B TRANSMITTER AND RECEIVER DIMENSIONS

### B.1 TRANSMITTER

#### B.1.1 BLS450 TRANSMITTER

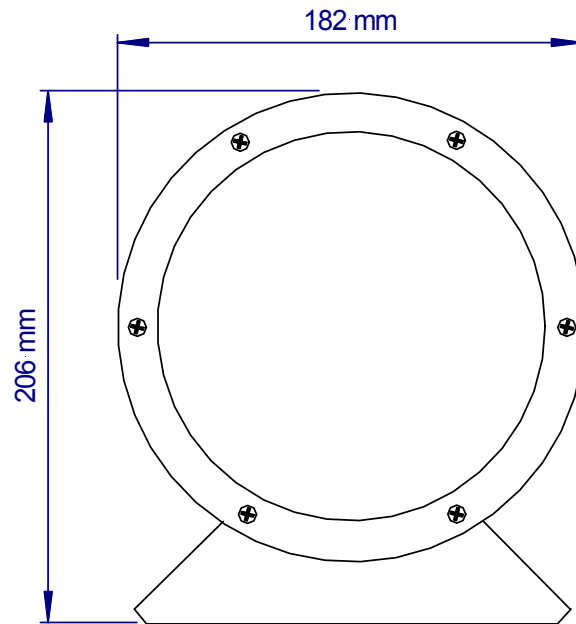


Figure 26: BLS450 Transmitter – Front View

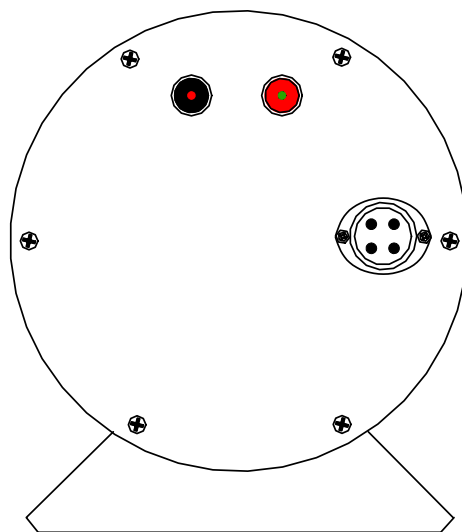


Figure 27: BLS450 Transmitter – Rear View

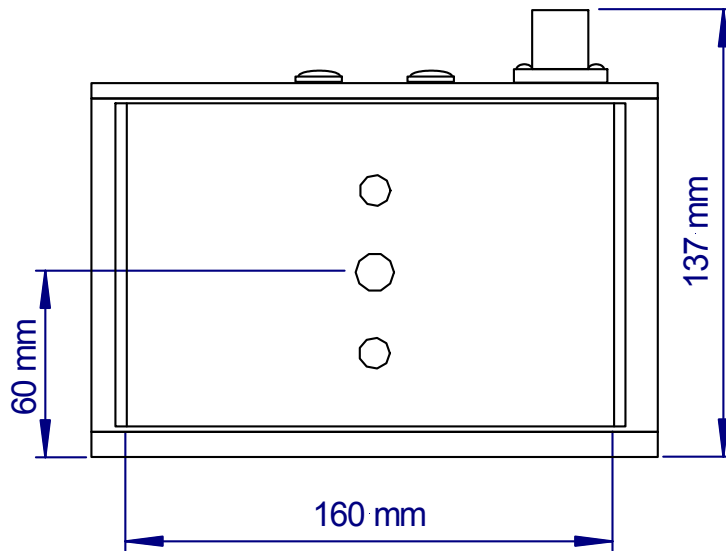


Figure 28: BLS450 Transmitter – Bottom View

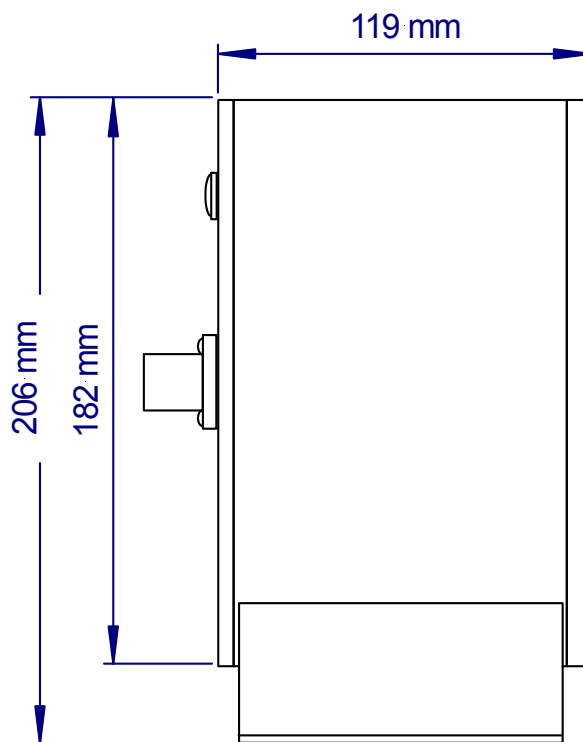


Figure 29: BLS450 Transmitter – Side View

## B.1.2 BLS900 TRANSMITTER

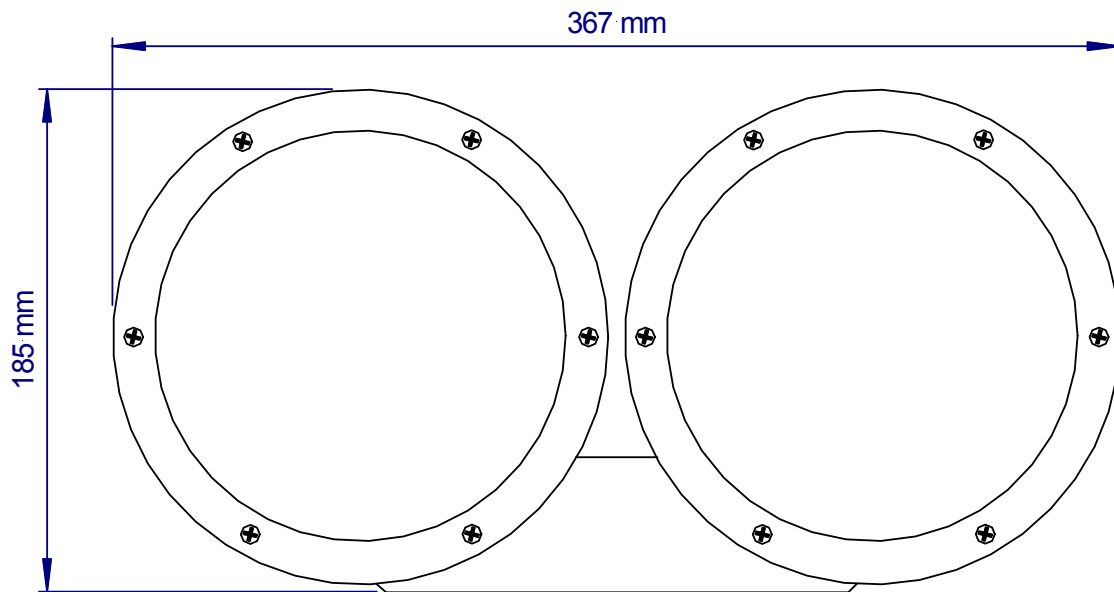


Figure 30: BLS900 Transmitter – Front View

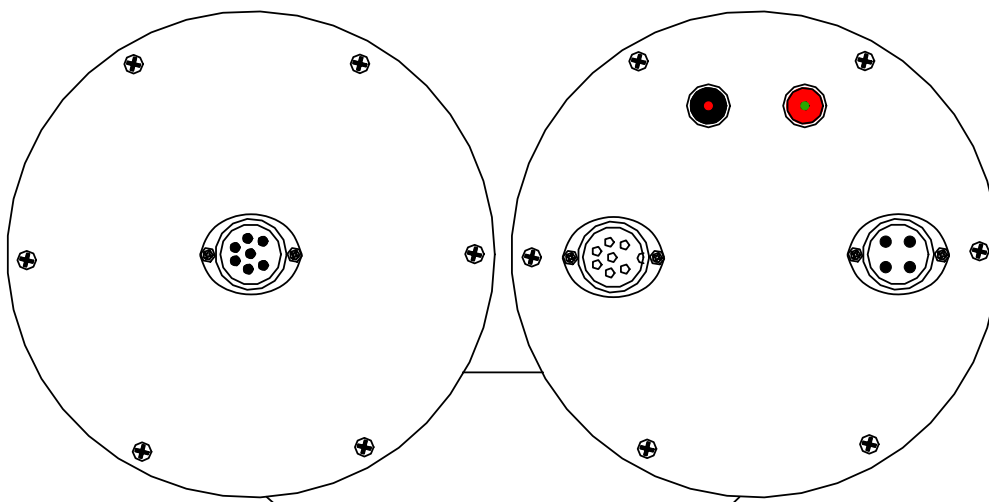


Figure 31: BLS900 Transmitter – Rear View

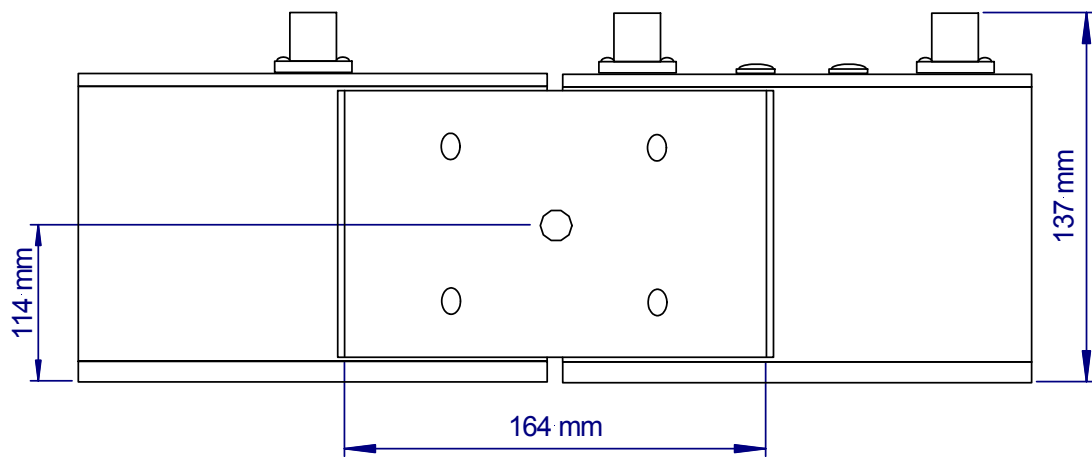


Figure 32: BLS900 Transmitter – Bottom View

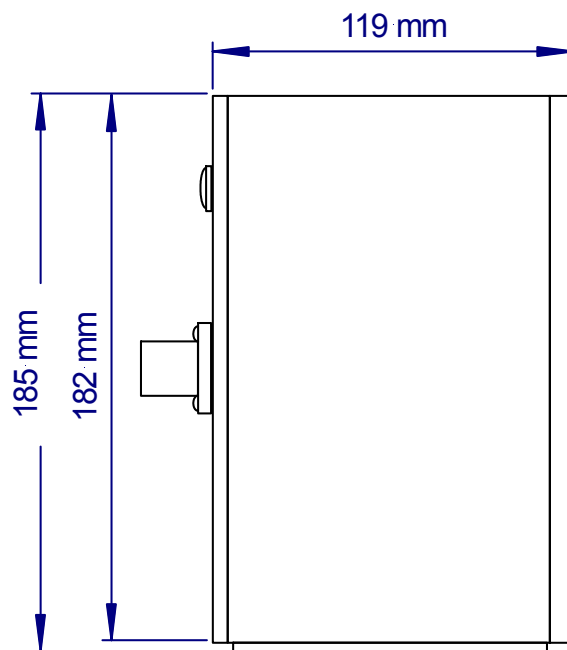


Figure 33: BLS900 Transmitter – Side View

### B.1.3 BLS2000 TRANSMITTER

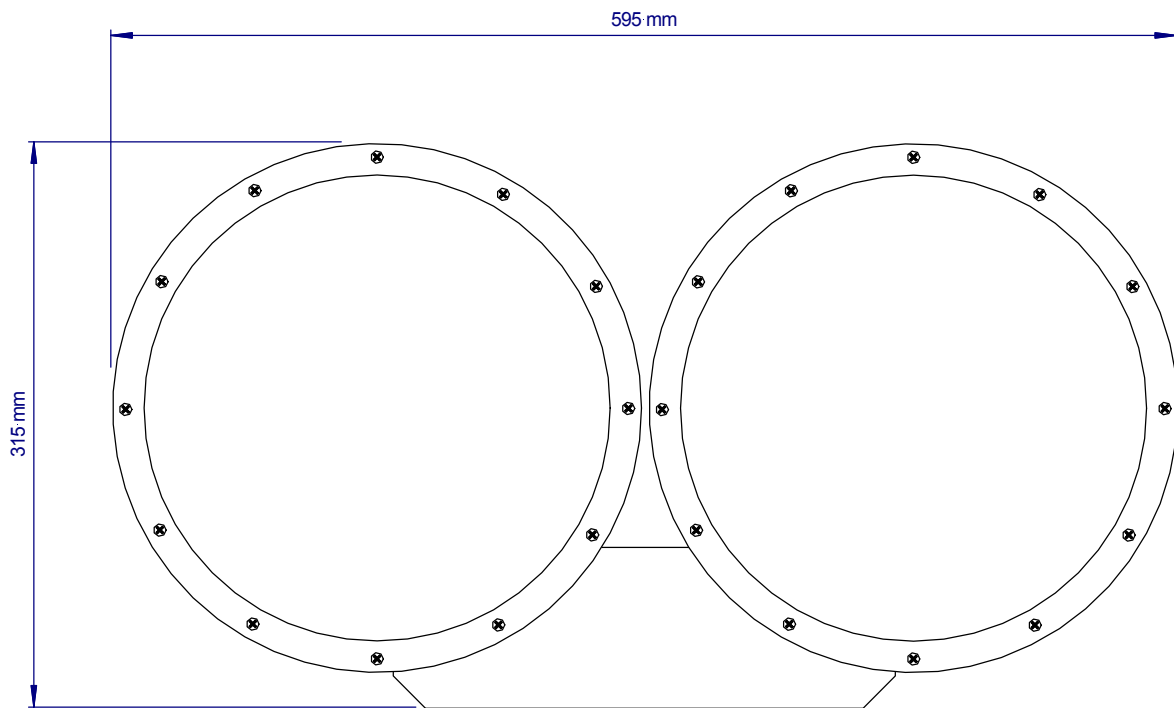


Figure 34: BLS2000 Transmitter – Front View

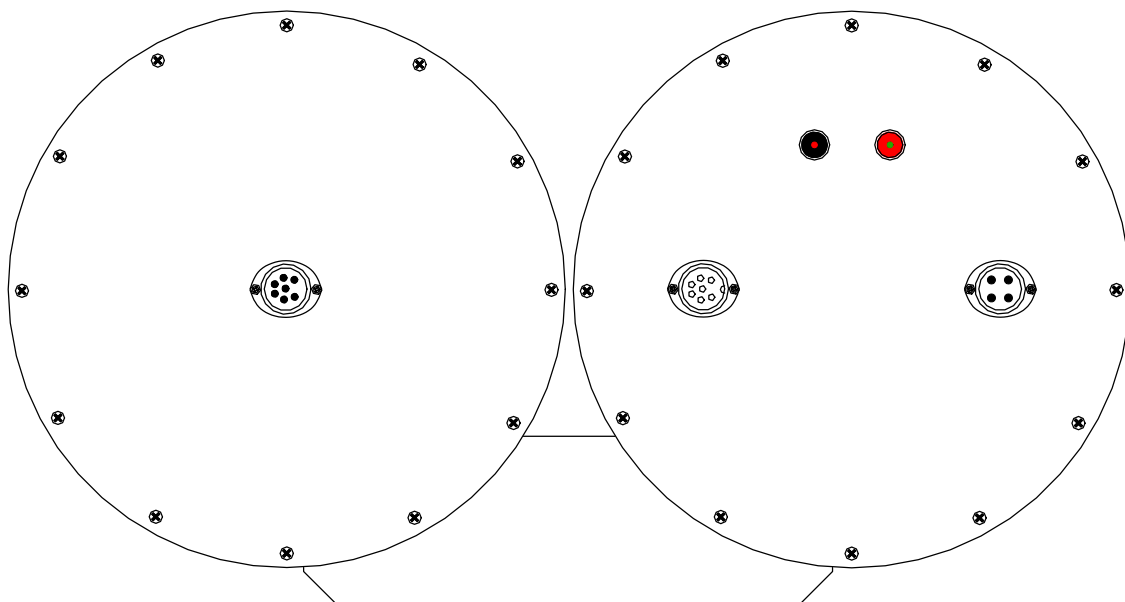


Figure 35: BLS2000 Transmitter – Rear View

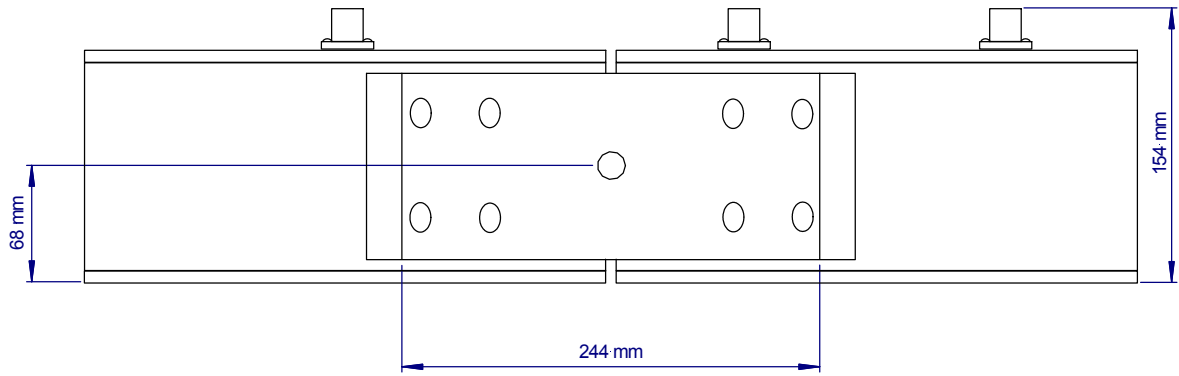


Figure 36: BLS2000 Transmitter – Bottom View

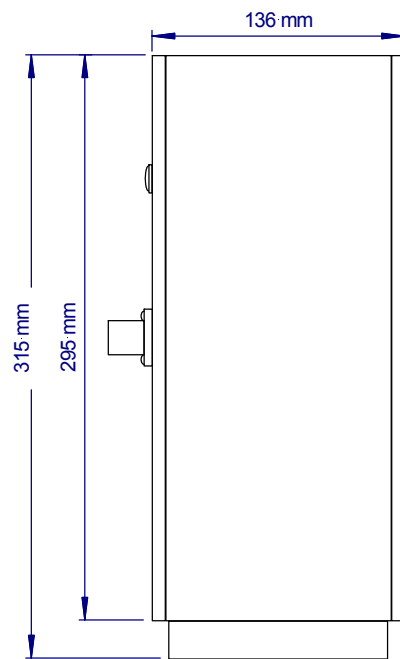


Figure 37: BLS2000 Transmitter – Side View

---

## B.2 RECEIVER

### B.2.1 BLS450 / BLS900 RECEIVER

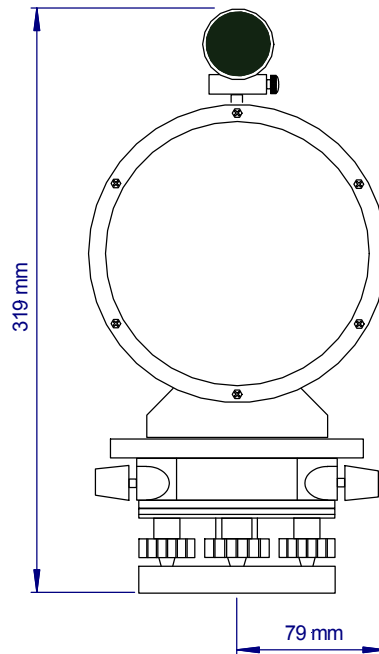


Figure 38: BLS450 / BLS900 Receiver – Front View

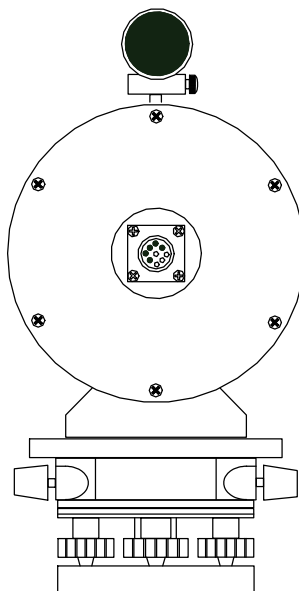


Figure 39: BLS450 / BLS900 Receiver– Rear View

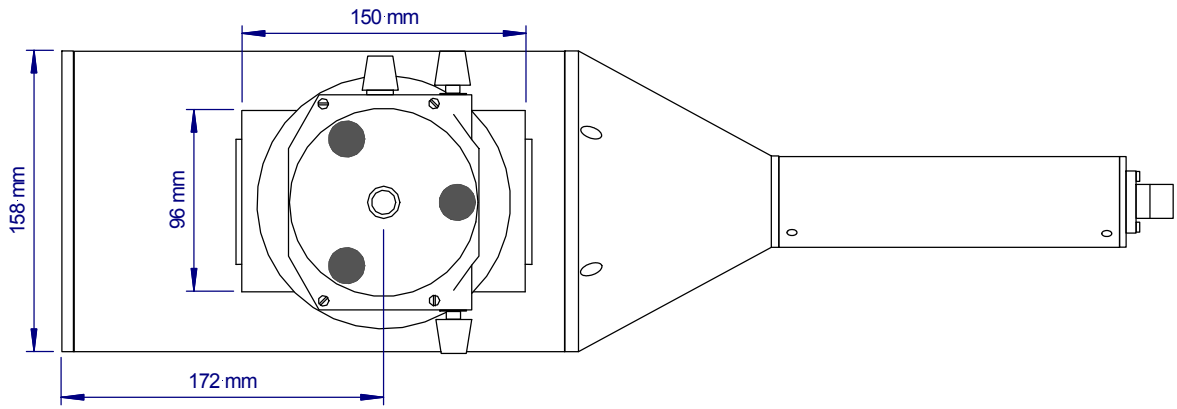


Figure 40: BLS450 / BLS900 Receiver – Bottom View

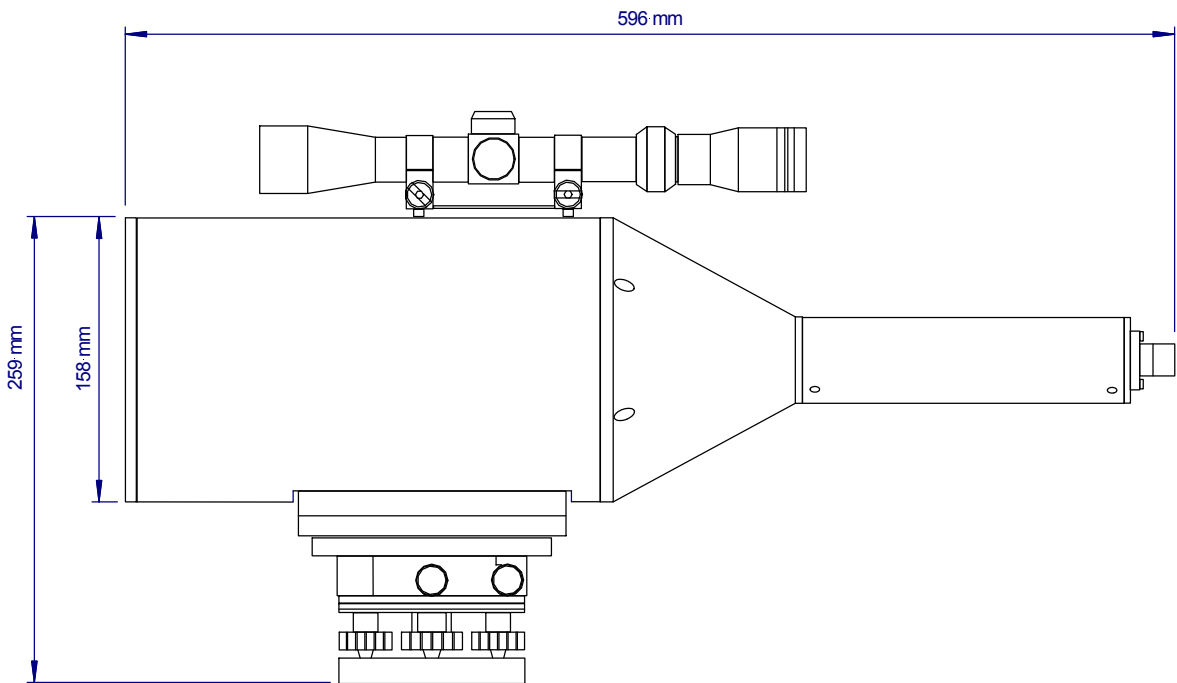


Figure 41: BLS450 / BLS900 Receiver – Side View

## B.2.2 BLS2000 RECEIVER

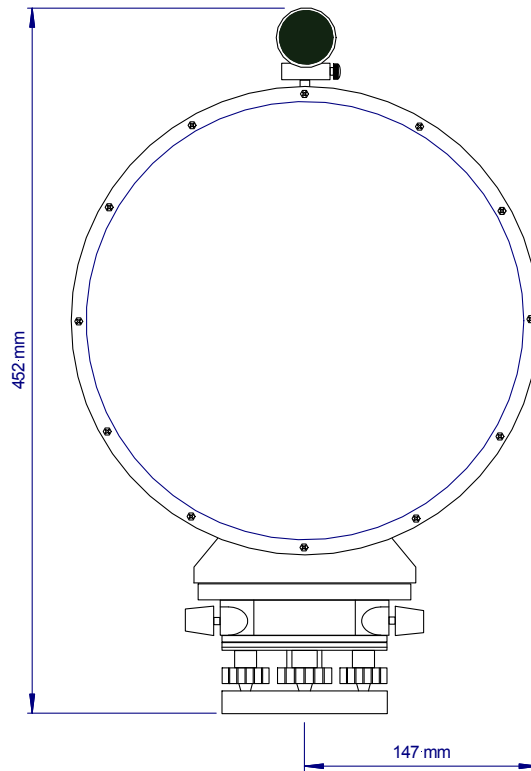


Figure 42: BLS2000 Receiver – Front View

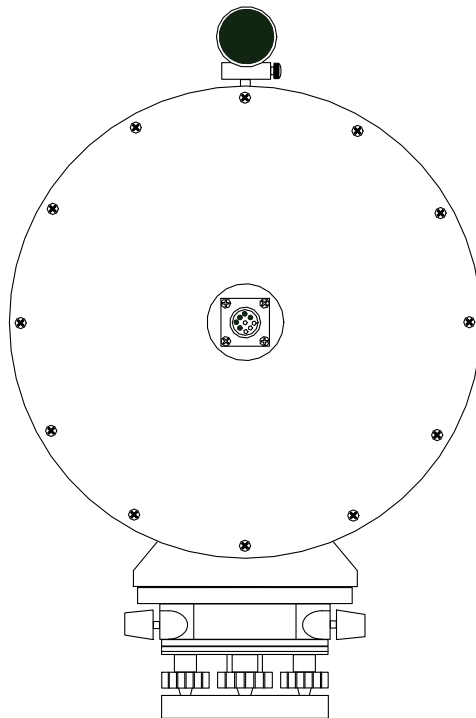


Figure 43: BLS2000 Receiver– Rear View

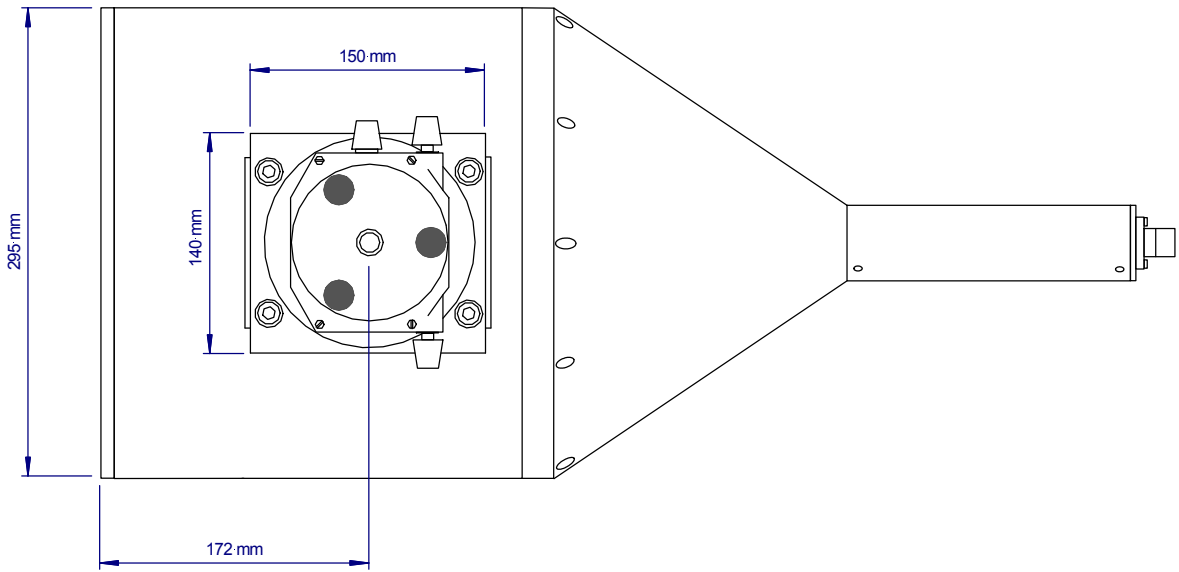


Figure 44: BLS2000 Receiver – Bottom View

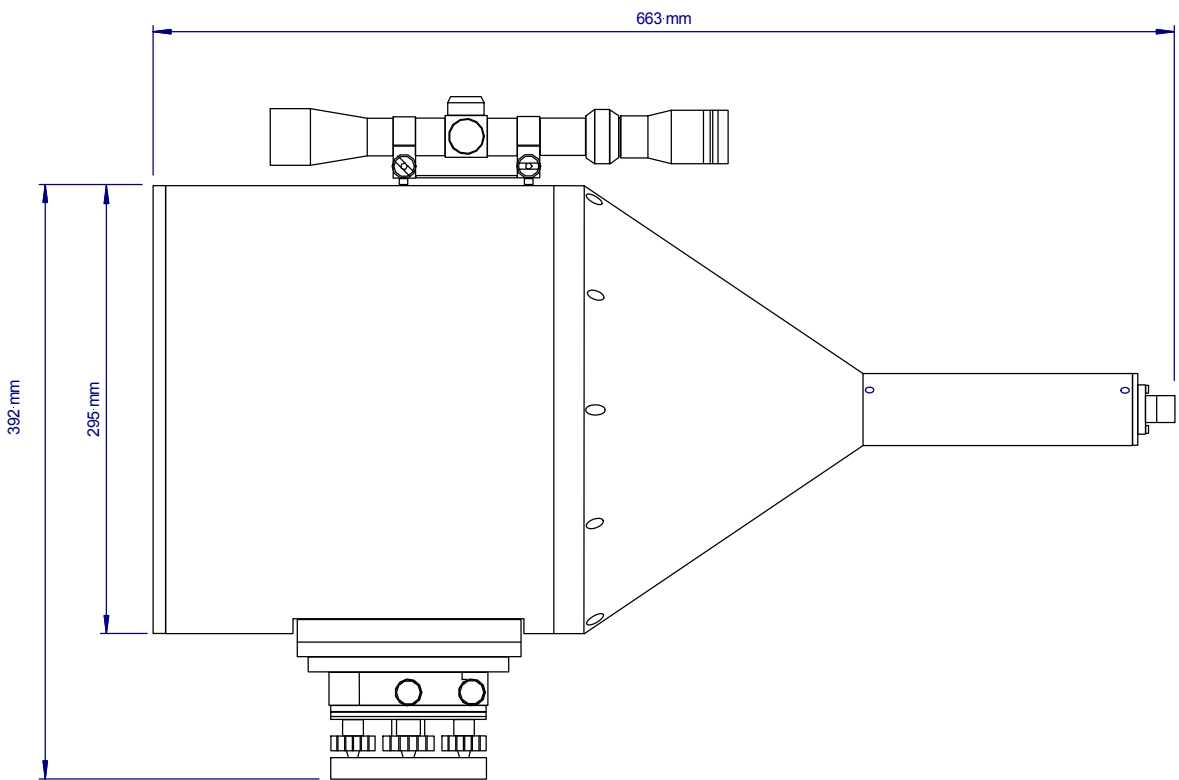


Figure 45: BLS2000 Receiver – Side View

## APPENDIX C SPECIFICATIONS

### C.1 TRANSMITTER

Specifications	BLS450	BLS900	BLS2000	Remarks
Main radiation source	444 LEDs GaAIAs	888 GaAIAs LEDs	1756GaAIAs LEDs	Infrared
Degradation time MTTF	55 000 hours	55 000 hours	55 000 hours	With PRR= 125 HZ
Auxiliary radiation source	18 LEDs visible	36 LEDs	68 LEDs	Red
Maximal optical power	7.5 W	15 W	28 W	
Wavelength	880 nm	880 nm	880 nm	$\Delta\lambda = \pm 20$ nm
Beam Divergence	16°	16°	16°	Full width half max
Pulse Repetition Rates (PRR)	1Hz, 5Hz, 25 Hz, 125Hz	1Hz, 5Hz, 25 Hz, 125Hz	1Hz, 5Hz, 25 Hz, 125Hz	$\pm 5\%$
Pulse length	8 ms	8 ms	8 ms	
Modulation frequency	1750 Hz	1750 Hz and 2500 Hz	1750 Hz and 2500 Hz	
Operation voltage	12 VDC	12 VDC	12 VDC	Max. Voltage 15 VDC
Power consumption	40 W 8 W 2 W 1 W	80 W 16 W 4 W 1 W	150 W 30 W 70 W 2 W	PRR=125 Hz PRR= 25Hz PRR= 5Hz PRR= 1Hz
Dimensions	180 x 180 x 135 mm	364 x 180 x 135 mm	590 x 330 x 170 mm	
Weight	4.5 kg	8.5 kg	22 kg	

Table 6: Specifications of BLS Transmitter

## C.2 RECEIVER

Specifications	BLS450 and BLS900	BLS2000	Remarks
Lens	Plan convex	Fresnel, plan	
Focal length	450 mm	495 mm	
Diameter	145 mm	265 mm	
Field of view	8 mrad	7.5 mrad	
Detectors	2 Si Photodiodes	2 Si Photodiodes	
Sensitive area	15 mm <sup>2</sup>	15 mm <sup>2</sup>	Signal 1
Sensitive area	5 mm <sup>2</sup>	5 mm <sup>2</sup>	Signal 2
Dimension	Ø160 x 590 mm	570 x 480 x 300 mm	
Weight	7.6 kg	19 kg	

Table 7: Specifications of BLS Receiver

## C.3 SPU

Specifications	BLS450, BLS900, BLS2000	Remarks
Integration time	1 min	
Data Storage Capacity	Approx. 2 years	Between data downloads, without raw data storage. Non-volatile flash storage
Internal clock	Date and time	
Operation temperature range	-20°C ~ + 50°C	
Operation voltage	12 VDC	Maximum voltage :15 VDC
Weight	8.0 kg	
Dimension	330 x 230 x 180 mm	
Power consumption (including Receiver)	20 W	Independent of PRR
Power consumption BLS2000 Heating	9.6 W	

Table 8: Specifications of BLS SPU

---

## C.4 BLS POWER SUPPLY

Specifications	BLS450, BLS900, BLS2000	Remarks
Output voltage	15 VDC	
Output current	8.5 A	
Weight	10 kg	
Dimension	230 x 200 x 180 mm	

Table 9: Specifications of BLS Power Supply

## C.5 BLS UPS

Specifications	BLS450, BLS900, BLS2000	Remarks
Input voltage	15 VDC	when connected to BLS Power Supply
Output voltage	11 VDC to max. 14 VDC	
Output current	10 A	
Capacity	40 Ah	
Weight	23 kg	
Dimension	400 x 230 x 225 mm	

Table 10: Specifications of BLS UPS

---

## APPENDIX D DECLARATION OF CONFORMITY

Name and address of manufacturer:

Scintec AG  
Wilhelm-Maybach-Str. 14  
72108 Rottenburg  
Germany

We declare that the products

**Boundary Layer Scintillometer, Models BLS450, BLS900, BLS2000**

comply with the Electromagnetic Compatibility Regulations (EMC) and, as far as applicable, the Low Voltage Directive (LVD) of the European Community.

Conformity is guaranteed for delivered complete systems and independently operable components. This declaration does not refer to systems resulting from an integration of external components such as data loggers, PC's, power supplies, cables, etc. by others than the manufacturer.

Applicable norms and standards:

EN 50081-1 (EMC Generic Standard - Radiated and Conducted Emissions)  
EN 55014 (EMC Product Standard - Radiated and Conducted Emissions)  
EN 55022 Class B (EMC Product Standard (IT) – Radiated and Conducted Emissions)

EN 50082-1 (EMC Generic Standard - Radiated and Conducted Immunity)  
EN 60555-2, 60555-3 (EMC Product Standard - Radiated and Conducted Immunity)  
EN 55024 / IEC 801-1 - 801-6 (EMC Product Standard (IT) – Radiated and Conducted Immunity)











